Pathology International 2010; **60**: 291–297 doi:10.1111/j.1440-1827.2010.02519.x

Original Article

Immunostaining of gastric cancer with neuroendocrine differentiation: Reg IV-positive neuroendocrine cells are associated with gastrin, serotonin, pancreatic polypeptide and somatostatin

Kazuhiro Sentani,[1] Naohide Oue,[1] Tsuyoshi Noguchi,[2] Naoya Sakamoto,[1] Keisuke Matsusaki[3] and Wataru Yasui[1]

[1]*Department of Molecular Pathology, Hiroshima University Graduate School of Biomedical Sciences, Hiroshima,* [2]*Department of Gastrointestinal Surgery, Oita University Faculty of Medicine, Oita and* [3]*Department of Surgery, Hofu Institute of Gastroenterology, Hofu, Japan*

We previously reported that Reg IV is associated with neuroendocrine (NE) differentiation in gastric cancers. The aim was to examine which NE hormone products are related to Reg IV-positive NE cells and their roles in gastric cancers. In the present study, we performed immunohistochemical analysis in a tissue microarray (TMA) of a consecutive series of 630 cases with ten different antibodies, including chromogranin A, synaptophysin and neural cell adhesion molecule (NCAM) as NE differentiation markers, and gastrin, serotonin, calcitonin, gastrin-releasing peptide (GRP), pancreatic polypeptide (PP), somatostatin and glucagon as NE hormones. In 630 cases, we identified 205 (33%) with NE differentiation and 147 (23%) positive for Reg IV. Reg IV-positive cases showed NE differentiation more frequently than Reg IV-negative cases ($P < 0.0001$). In 205 cases with NE differentiation, Reg IV-positive cases expressed serotonin ($P = 0.0032$) and somatostatin ($P = 0.036$) more frequently than Reg IV-negative cases. Double immunofluorescence staining revealed co-expression of Reg IV with gastrin, serotonin and PP. These results indicate that Reg IV might be a mediating factor of several NE hormones.

Key words: gastric cancer, gastrin, neuroendocrine differentiation, Reg IV, serotonin

The presence of neuroendocrine (NE) differentiation in gastric carcinoma has been relatively well studied, with occurrences varying from 19% to 53% in the literature reported.[1,2] Neuroendocrine cells are found interspersed among adenocarcinoma cells in typical gastric cancers,[3,4] which must be distinguished from NE carcinomas with highly malignant biological behavior and extremely poor prognosis.[5] The clinical significance of NE differentiation in gastric cancer in general is still controversial, with reports of a better[6] and also a poorer associated prognosis.[1] On the other hand, NE neoplasms are varied in their biological behavior, depending on their cell type, and can produce different NE hormones causing distinct clinical endocrine syndromes.[7] Compared with NE carcinomas, little investigation has been carried out on the direct relationship between NE cells and their NE hormone products in non-NE cancers, especially in common gastric cancers.[6,8,9]

We previously performed serial analysis of gene expression (SAGE) of primary gastric cancers[10] and identified several gastric cancer-related genes[11] and useful diagnostic markers.[12] Of these genes, *Regenerating islet-derived family, member 4* (*REG4*, which encodes Reg IV) is a candidate gene for cancer-specific expression.[11] *REG4* is a member of the REG gene family, which includes three other genes, and was originally identified by high-throughput sequence analysis of a large inflammatory bowel disease cDNA library.[13] By quantitative reverse transcription polymerase chain reaction (RT-PCR) and immunohistochemical analysis, overexpression of Reg IV was detected in 30–50% of gastric cancers.[10] Reg IV is also expressed in colorectal cancer,[14] pancreatic cancer,[15] prostate cancer,[16] and adenoid cystic carcinoma.[17] Immunohistochemically, there are two Reg IV staining patterns; mucin-like staining and perinuclear staining.[18] Mucin-like staining, observed in goblet cells and goblet cell-like vesicles of tumor cells, is associated with MUC2 (a marker of

Correspondence: Wataru Yasui, MD, PhD, Department of Molecular Pathology, Hiroshima University Graduate School of Biomedical Sciences, 1-2-3 Kasumi, Minami-ku, Hiroshima 734-8551, Japan. Email: wyasui@hiroshima-u.ac.jp

Received 7 October 2009. Accepted for publication 9 December 2009.

Table 1 Antibodies used in the current study

Antigen	Clone	Dilution	Pretreatment	Source
Reg IV	Polyclonal	1:50	MW	†
Chromogranin A	Polyclonal	1:50	MW	Novocastra, Newcastle on Tyne, UK
Synaptophysin	Polyclonal	1:50	MW	DAKO, Carpinteria, CA, USA
NCAM	1B6	1:50	MW	Novocastra, Newcastle on Tyne, UK
Gastrin	Polyclonal	1:50	MW	Santa Cruz Biotechnology, Santa Cruz, CA, USA
Serotonin	5HT-H209	1:50	MW	DAKO, Carpinteria, CA, USA
Calcitonin	Polyclonal	1:50	MW	Novocastra, Newcastle on Tyne, UK
GRP	H-027-07	1:50	MW	Phoenix pharmaceuticals, Burlingame, CA, USA
PP	H-054-02	1:50	MW	Phoenix pharmaceuticals, Belmont, CA, USA
Somatostatin	Polyclonal	1:50	MW	DAKO, Carpinteria, CA, USA
Glucagon	Polyclonal	Diluted	MW	Nichirei, Tokyo, Japan

†Rabbit polyclonal anti-Reg IV antibody was raised in our laboratory.

GRP, gastrin-releasing peptide; NCAM, neural cell adhesion molecule; PP, pancreatic polypeptide; MW, microwaving (500W) in citrate buffer (pH 6.0) for 15 min.

goblet cells) positivity. Perinuclear staining is detected in cells with NE differentiation. However, it remains unclear which NE hormone products are related to Reg IV-positive NE cells.

In the present study, to characterize Reg IV-positive NE cells, immunohistochemical examination was carried out in a tissue microarray (TMA) of a consecutive series of 630 gastric cancers with ten different antibodies, including chromogranin A, synaptophysin and neural cell adhesion molecule (NCAM) as NE differentiation markers, and gastrin, serotonin, calcitonin, gastrin-releasing peptide (GRP), pancreatic polypeptide (PP), somatostatin and glucagon as NE hormones.

MATERIALS AND METHODS

Tissue samples and TMA construction

The surgical pathology files of the Hiroshima University Hospital, Japan, and its affiliated hospitals were used to randomly select 630 cases of gastric cancer. Surgically resected specimens were routinely fixed in 10% buffered formalin and examined macroscopically. Tumor staging was performed according to the Union Internationale Contre le Cancer (UICC) system.[19] Histological classification was carried out according to the Lauren classification system.[20] There were 112 Tis, 155 T1, 208 T2, 123 T3, and 32 T4 in these 630 cases. Nodal metastasis was present in 285 patients (45%). Tumor staging revealed 112 stage 0, 227 stage I, 113 stage II, 113 stage III, and 65 stage IV. Gastric cancers were histologically classified as 357 intestinal type and 273 diffuse type cancers. In accordance with the Ethical Guidelines for Human Genome/Gene Research enacted by the Japanese Government, tissue specimens were collected and used after approval from the Ethical Review Committee of the Hiroshima University School of Medicine and from the ethical review committees of collaborating organizations.

The two most representative tumor areas to be sampled for the TMAs were carefully selected and marked on the hematoxylin & eosin (HE)-stained slide in each case. Two superficial areas in mucosal gastric cancers, and one superficial area and one deep area in gastric cancers that had invaded punched out and transferred to a recipient block with a maximum of 48 cores using a Tissue Microarrayer (AZUMAYA KIN-1, Tokyo, Japan). Five-μm-thick sections were cut from the recipient block and transferred to glass slides. HE staining was performed on TMA for confirmation of the tumor tissue. Each tissue-array block contained 21 cases of gastric cancer and four cases of non-neoplastic stomach samples.

Immunohistochemistry

A Dako Envision Kit (DAKO, Carpinteria, CA, USA) was used for immunohistochemical analysis of all markers except gastrin. In brief, sections were pretreated by microwaving (500W) in citrate buffer (pH 6.0) for 15 min to retrieve antigenicity. After endogenous peroxidase activity was blocked with 3% H_2O_2-methanol for 10 min, sections were incubated with normal goat serum (DAKO) for 20 min to block non-specific antibody binding sites. Sections were then incubated with the following primary antibodies (Table 1): anti-Reg IV, anti-chromogranin A, anti-synaptophysin, anti-NCAM, anti-gastrin, anti-serotonin, anti-calcitonin, anti-GRP, anti-PP, anti-somatostatin, and anti-glucagon. Suppliers and working dilutions are noted in Table 1. Rabbit polyclonal anti-Reg IV antibody was raised in our laboratory.[18] The specificity of the Reg IV antibody has been characterized in detail.[18] Sections were incubated with primary antibody for 1 h at 25°C, followed by incubations with peroxidase-labeled anti-rabbit or mouse IgG for 60 min. For immunostaining of gastrin, peroxidase-conjugated anti-goat IgG was used as the secondary antibody. Staining was completed with a 10-minute incubation

with the substrate-chromogen solution. The sections were counterstained with 0.1% hematoxylin. Appropriate positive and negative control samples were used.

Double-immunofluorescence staining was performed as described previously.[21] Alexa Fluor 546-conjugated anti-goat IgG (Molecular Probes, Eugene, OR, USA) and Alexa Fluor 488-conjugated anti-rabbit IgG (Molecular Probes) or Alexa Fluor 546-conjugated anti-mouse IgG (Molecular Probes) and Alexa Fluor 488-conjugated anti-rabbit IgG (Molecular Probes) were used as secondary antibodies.

Evaluation of positive cases and cutoff-point thresholds

Immunostaining was evaluated independently by two investigators (KS, NO), and when the evaluations differed, a decision was made by consensus while investigators reviewed the specimen with a multihead microscope. Neoplastic tissue was evaluated semiquantitatively at magnifications of ×100 and ×400. Cytoplasmic immunoreactivity for Reg IV, chromogranin A, synaptophysin, gastrin, serotonin, calcitonin, GRP, PP, somatostatin, and glucagon; and membranous reactivity for NCAM were assessed.

For the TMAs, staining was considered positive if any tumor cells were stained appropriately. The percentage of reactive cells necessary for a positive result reflects the viewpoint and opinion of the authors. There can be significant methodologic differences between studies and we are aware of the potential effect of these differences on a study's results. The aim of the present study was to analyze the presence or absence of various NE markers in gastric cancers. Therefore, the cutoff-point for antibody reactivity necessary to define a result as positive was staining of any (>0%) cells in the TMAs.

Statistical methods

Associations between clinicopathologic variables and immunostaining for neuroendocrine markers were analyzed by Fisher's exact test. A *P*-value less than 0.05 was considered statistically significant.

RESULTS

Association between various NE markers and Reg IV in non-neoplastic gastric mucosa

In non-neoplastic gastric mucosa, all NE hormones examined, except GRP, were detected in both intestinal metaplasia and non-metaplastic gastric mucosa, whereas GRP was expressed only in non-metaplastic gastric mucosa. In intestinal metaplasia, goblet cells showed Reg IV expression in goblet cell vesicles (Fig. 1a). In addition, NE cells at the base of intestinal metaplasia displayed Reg IV staining in the perinuclear region (Fig. 1a). As reported previously, cells with Reg IV staining of the perinuclear region are NE cells; however, all NE cells are not always positive for Reg IV. In non-metaplastic gastric mucosa, Reg IV staining was not observed. The distribution of Reg IV staining was compared with the distribution of NE hormone staining in serial sections. Some Reg IV-positive NE cells expressed gastrin, serotonin, and PP. Double immunofluorescence staining revealed co-expression of Reg IV with gastrin (Fig. 2a), serotonin (Fig. 2b), and PP (not shown). However, there were several NE cells that were positive for Reg IV but not for gastrin, serotonin, or PP, and vice versa. Co-expression of Reg IV with the other NE hormones was not observed (data not shown).

Expression of various NE markers in gastric cancers and their correlation with clinicopathologic parameters

Of the 630 gastric cancers, 147 (23%) were identified as Reg IV-positive. NE markers detected in the 630 cases included 76 (12%) cases with chromogranin A, 157 (25%) cases with synaptophysin, and 11 (2%) cases with NCAM. A total of 205 (33%) cases were found to have NE differentiation, and Reg IV-positive cases showed NE differentiation more frequently than Reg IV-negative cases ($P < 0.0001$). The incidence of gastric cancer with production of NE hormones was 4% for gastrin, 3% for serotonin, 2% for calcitonin, 9% for GRP, 5% for PP, 3% for somatostatin, and 1% for glucagon. We investigated the relation between the expression of various NE markers and their clinicopathologic parameters. As shown in Table 2, the expression of synaptophysin, gastrin, and GRP was associated with intestinal type according to Lauren classification ($P = 0.0414$, 0.0281, and 0.0208). Positive expression of Reg IV, chromogranin A, and gastrin were significantly more frequent in gastric cancers of Tis/T1 than those in T2/3/4 ($P = 0.0057$, 0.0351, and 0.024). Furthermore, gastrin-positive cases were significantly more frequent in stage 0/I cases than stage II/III/IV cases ($P = 0.0105$). In contrast, no correlation was found between other NE markers (NCAM, serotonin, calcitonin, PP, somatostatin, and glucagons) and clinicopathologic parameters.

We further analyzed association between Reg IV and various NE hormones in gastric cancers. Of 147 Reg IV-positive cases, 63 (43%) showed both mucin-like staining and perinuclear staining (Fig. 1b), whereas the remaining 84 (57%) displayed only mucin-like staining. Gastric cancers showing only perinuclear staining were not found. Therefore, of 630 gastric cancers, 63 cases showed perinuclear Reg IV

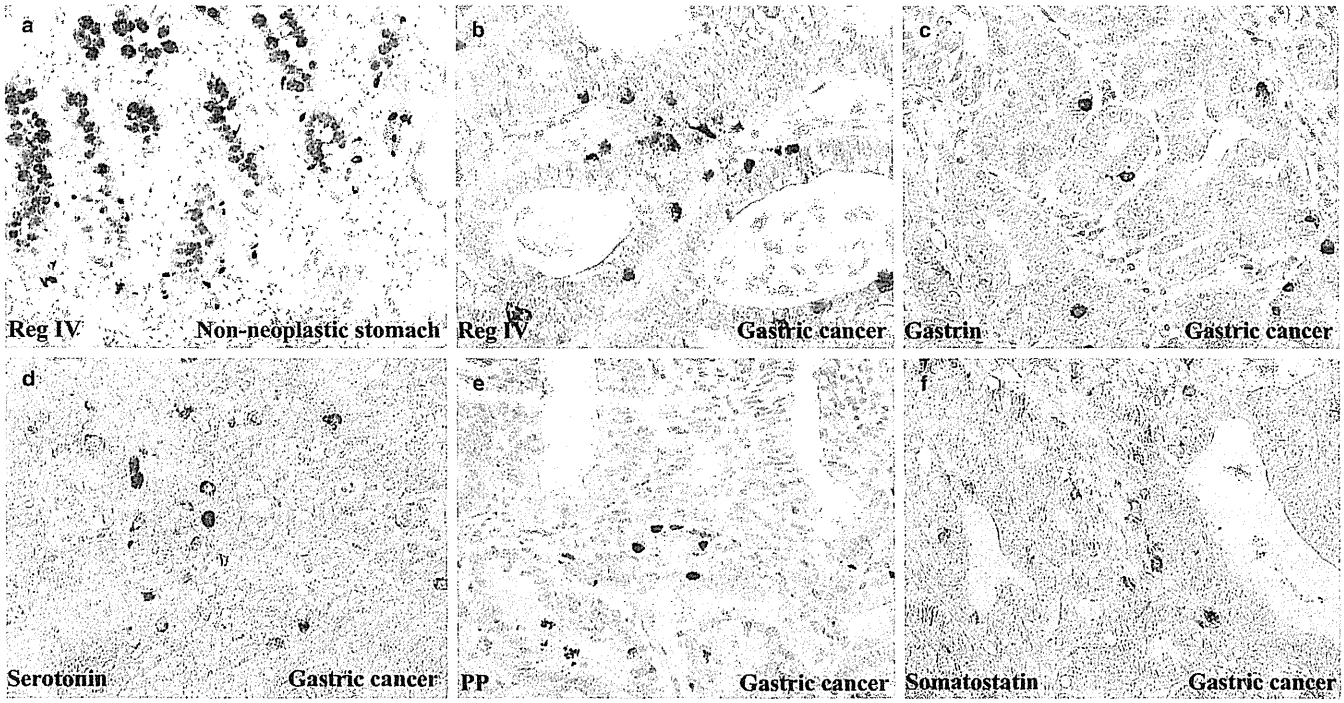

Figure 1 Immunohistochemical staining of Reg IV and neuroendocrine (NE) hormones. Reg IV showed positive staining in both goblet cell vesicles in goblet cells and the perinuclear region of neuroendocrine cells at the base of intestinal metaplasia (**a**). Reg IV showed positive staining in the perinuclear region of gastric cancer (**b**). Some gastric cancer cells showed production of NE hormones such as gastrin (**c**), serotonin (**d**), pancreatic polypeptide (PP) (**e**) and somatostatin (**f**).

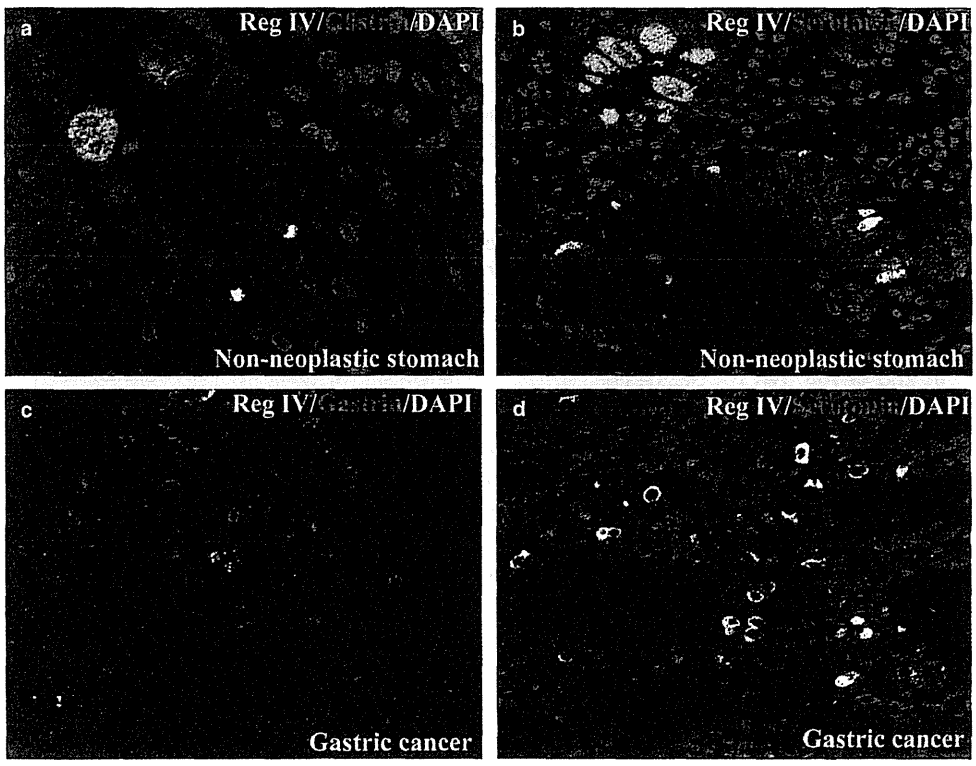

Figure 2 Double immunofluorescence staining revealed some non-neoplastic stomach cells with co-expression between Reg IV and gastrin (**a**), and Reg IV and serotonin (**b**). Some gastric cancer cells showed co-expression between Reg IV and gastrin (**c**), and Reg IV and serotonin (**d**). Cells were imaged with a fluorescence microscope as described in the Methods.

Table 2 Expression of various NE markers in gastric cancers and its correlation with clinicopathologic parameters

Histology† & TNM status	Reg IV	Chromogranin A	Synaptophysin	NCAM	Gastrin	Serotonin
Histology						
Intestinal type	85 (24%)	48 (13%)	100 (28%)	6 (2%)	21 (5%)	14 (3%)
Diffuse type	62 (23%)	28 (10%)	57 (21%)	5 (2%)	6 (2%)	7 (2%)
P-value	NS	NS	0.0414	NS	0.0281	NS
T grade						
Tis/T1	77 (29%)	41 (15%)	68 (25%)	4 (1%)	18 (6%)	10 (4%)
T2/T3/T4	70 (19%)	35 (10%)	89 (25%)	7 (2%)	9 (2%)	11 (3%)
P-value	0.0057	0.0351	NS	NS	0.0240	NS
N grade						
N0	87 (25%)	47 (14%)	87 (25%)	3 (0.9%)	18 (5%)	12 (3%)
N1/2/3	60 (21%)	29 (10%)	70 (25%)	8 (3%)	9 (3%)	9 (3%)
P-value	NS	NS	NS	NS	NS	NS
Staging						
Stage 0/I	89 (26%)	48 (14%)	88 (26%)	5 (1%)	21 (6%)	11 (3%)
Stage II/III/IV	58 (20%)	28 (10%)	69 (24%)	6 (2%)	6 (2%)	10 (3%)
P-value	NS	NS	NS	NS	0.0105	NS

Histology† & TNM status	Calcitonin	GRP	PP	Somatostatin	Glucagon
Histology					
Intestinal type	4 (1%)	39 (10%)	24 (6%)	11 (3%)	4 (1%)
Diffuse type	9 (3%)	15 (5%)	10 (3%)	5 (1%)	1 (0.4%)
P-value	NS	0.0208	NS	NS	NS
T grade					
Tis/T1	4 (1%)	28 (10%)	19 (7%)	7 (3%)	3 (1%)
T2/T3/T4	9 (2%)	26 (7%)	15 (4%)	9 (2%)	2 (0.6%)
P-value	NS	NS	NS	NS	NS
N grade					
N0	8 (2%)	31 (9%)	23 (7%)	9 (3%)	4 (1%)
N1/2/3	5 (2%)	23 (8%)	11 (4%)	7 (2%)	1 (0.4%)
P-value	NS	NS	NS	NS	NS
Staging					
Stage 0/I	6 (2%)	32 (9%)	22 (6%)	8 (2%)	4 (1%)
Stage II/III/IV	7 (2%)	22 (8%)	12 (4%)	8 (3%)	1 (0.3%)
P-value	NS	NS	NS	NS	NS

†Histologic classification was carried out according to the Lauren classification system. Tumor staging was performed according to the UICC system. GRP, gastrin-releasing peptide; NCAM, neural cell adhesion molecule; NE, neuroendocrine; NS, not significant; PP, pancreatic polypeptide.

staining. In contrast, 205 (33%) of 630 cases showed NE differentiation. All 63 gastric cancers with perinuclear Reg IV staining showed NE differentiation. To characterize Reg IV-positive NE cells, we focused on only gastric cancers showing perinuclear Reg IV staining. In 205 cases with NE differentiation, expression of serotonin was more frequently detected in Reg IV-positive cases (10/63, 16%) than in Reg IV-negative cases (5/142, 4%, $P = 0.0032$) (Table 3). In addition, expression of somatostatin was more frequently found in Reg IV-positive cases (8/63, 13%) than in Reg IV-negative cases (6/142, 4%, $P = 0.0360$) (Table 3). Expressions of other NE hormones were not correlated with Reg IV expression (Table 3). Next, the distribution of Reg IV staining was compared with the distribution of NE hormone staining in serial sections (Fig. 1c–f). Some Reg IV-positive cancer cells expressed gastrin, serotonin, and PP. Double immunofluorescence staining revealed co-expression of Reg IV with gastrin (Fig. 2c), serotonin (Fig. 2d), and PP. However, there were several cancer cells that were positive for Reg IV but not gastrin, serotonin, or PP, and vice versa. Co-expression of Reg IV with the other NE hormones was not observed (data not shown).

Table 3 Association between Reg IV and various NE hormones in 205 gastric cancers with NE differentiation

	Reg IV		
	Positive (63)	Negative (142)	Total 205 cases
Gastrin (+)	9 (14%)	12 (8%)	$P = 0.2181$
Serotonin (+)	10 (16%)	5 (4%)	$P = 0.0032$
Calcitonin (+)	4 (6%)	4 (3%)	$P = 0.2534$
GRP (+)	16 (25%)	25 (18%)	$P = 0.2557$
PP (+)	11 (17%)	16 (11%)	$P = 0.2642$
Somatostatin (+)	8 (13%)	6 (4%)	$P = 0.036$
Glucagon (+)	0 (0%)	3 (2%)	$P = 0.5543$

GRP, gastrin-releasing peptide; NE, neuroendocrine; PP, pancreatic polypeptide.

DISCUSSION

In the previous study, we revealed that expression of Reg IV is associated with both intestinal and neuroendocrine differentiation.[18] Perinuclear Reg IV staining is detected in cells with NE differentiation; however, it remains unclear which NE hormone products are related to Reg IV-positive NE cells. In the present study, some Reg IV-positive NE cells were also positive for gastrin, serotonin, and PP in both non-neoplastic gastric mucosa and gastric cancer. Reg IV has been identified as one of the genes that has an important role in intestinal epithelium development, homeostasis and function.[22] Because Reg IV-positive cases showed NE differentiation more frequently than Reg IV-negative cases, Reg IV may play a certain role in NE differentiation.

Both mucin-like staining and perinuclear staining of Reg IV are detected in intestinal metaplasia. It is known that Cdx2, a mammalian caudal-related intestinal transcription factor, is important for the maintenance of intestinal epithelial cells.[23,24] In addition, several lines of evidence have suggested that intestinal metaplasia of the stomach and gastric cancer with the intestinal mucin phenotype are associated with ectopic Cdx2 expression.[25–27] Because Cdx2 interacts with the MUC2 promoter and activates MUC2 transcription,[28] Cdx2 may regulate transcription of the REGIV gene. The NE cells at the base of intestinal metaplasia displayed Reg IV staining in the perinuclear region. A possible link between intestinal metaplasia of the stomach and NE cells has been observed in neurogenin-3 knockout mice.[29] In these mice, intestinal metaplasia occurs in the stomach, and glucagons-secreting A-cells, somatostatin-secreting D-cells, and gastrin-secreting G-cells are absent, whereas the number of serotonin-expressing enterochromaffin cells is decreased but present. These data suggest that NE cells in intestinal metaplasia may have origins different from those of other NE cells. Because Reg IV-positive NE cells are present in intestinal metaplasia, Reg IV may be involved in differentiation of serotonin-expressing enterochromaffin cells. In the previous report,[14] we revealed that both perinuclear and mucin-like staining of Reg IV were detected in non-neoplastic colorectal mucosa, and these perinuclear Reg IV-positive cells also express chromogranin A. In contrast, only mucin-like staining of Reg IV was observed in colorectal cancers, and not perinuclear Reg IV staining. Therefore, we speculated that the effects of Reg IV on NE cells differ a little in each organ.

Although the biological function of Reg IV is poorly understood, it has been reported that Reg IV is a potent activator of the epidermal growth factor receptor (EGFR)/Akt/activator protein-1 (AP-1) signaling pathway in colon cancer cells and increases expression of Bcl2, Bcl-xl and survivin associated with the inhibition of apoptosis.[30] We have also reported that forced expression of Reg IV induces phosphorylation of the EGFR and inhibits 5-fluorouracil-induced apoptosis in gastric cancer.[31] In the present study, some Reg IV-positive NE cells were also positive for gastrin in both non-neoplastic gastric mucosa and gastric cancer. Gastrin increases the expression of the EGFR ligands such as amphiregulin and EGF,[32] augments cell proliferation as well as angiogenesis and metastasis, and reduces apoptosis.[33] Because Reg IV is expressed in almost all EGFR-positive gastric cancers,[31] both Reg IV and gastrin may activate EGFR and may contribute to cancer cell growth. In addition, gastrin-positive cases expressed somatostatin and GRP more frequently than gastrin-negative cases (data not shown). This is consistent with the previous report that gastrin release is controlled by somatostatin and GRP in a negative and positive manner, respectively.[34]

In the current study, Reg IV-positive cases showed NE differentiation more frequently than Reg IV-negative cases, and showed an inverse correlation with the depth of tumor invasion. Neuroendocrine hormones regulate homeostasis by affecting cell proliferation, differentiation, apoptosis, and gene expression. The aberrant control of these biological processes is thought to play an important role in the establishment of neoplasia.[35,36] Further analysis is required to examine how the combination of Reg IV and NE hormones participates in the regulation of tumor initiation and development.

ACKNOWLEDGMENTS

We thank Ms Emiko Hisamoto and Mr Masayuki Ikeda for their excellent technical assistance and advice. This work was carried out with the kind cooperation of the Research Center for Molecular Medicine, Faculty of Medicine, Hiroshima University. We thank the Analysis Center of Life Science, Hiroshima University, for the use of their facilities. This work was supported, in part, by Grants-in-Aid for Cancer Research from the Ministry of Education, Culture, Science, Sports and Technology of Japan; in part by a Grant-in-Aid for the Third Comprehensive 10-Year Strategy for Cancer Control and for Cancer Research from the Ministry of Health, Labour and Welfare of Japan.

REFERENCES

1 Ooi A, Mai M, Ogino T *et al.* Endocrine differentiation of gastric adenocarcinoma. The prevalence as evaluated by immunoreactive chromogranin A and its biologic significance. *Cancer* 1988; **62**: 1096–104.
2 Qvigstad G, Sandvik AK, Brenna E, Aase S, Waldum HL. Detection of chromogranin A in human gastric adenocarcinomas using a sensitive immunohistochemical technique. *Histochem J* 2000; **32**: 551–6.
3 Tahara E, Ito H, Nakagami K, Shimamoto F, Yamamoto M, Sumii K. Scirrhous argyrophil cell carcinoma of the stomach with

multiple production of polypeptide hormones, amine, CEA, lysozyme, and HCG. *Cancer* 1982; **49**: 1904–15.
4 Ito H, Hata J, Oda N, Miyamori S, Tahara E. Serotonin in tubular adenomas, adenocarcinomas and endocrine tumours of the stomach. An immunohistochemical study. *Virchows Arch A Pathol Anat Histopathol* 1986; **410**: 239–45.
5 Jiang SX, Mikami T, Umezawa A, Saegusa M, Kameya T, Okayasu I. Gastric large cell neuroendocrine carcinomas: A distinct clinicopathologic entity. *Am J Surg Pathol* 2006; **30**: 945–53.
6 Radi MJ, Fenoglio-Preiser CM, Bartow SA, Key CR, Pathak DR. Gastric carcinoma in the young: A clinicopathological and immunohistochemical study. *Am J Gastroenterol* 1986; **81**: 747–56.
7 Warner RR. Enteroendocrine tumors other than carcinoid: A review of clinically significant advances. *Gastroenterology* 2005; **128**: 1668–84.
8 Yao GY, Zhou JL, Lai MD, Chen XQ, Chen PH. Neuroendocrine markers in adenocarcinomas: An investigation of 356 cases. *World J Gastroenterol* 2003; **9**: 858–61.
9 Yasui W, Oue N, Sentani K *et al.* Transcriptome dissection of gastric cancer: Identification of novel diagnostic and therapeutic targets from pathology specimens. *Pathol Int* 2009; **59**: 121–36.
10 Oue N, Hamai Y, Mitani Y *et al.* Gene expression profile of gastric carcinoma: Identification of genes and tags potentially involved in invasion, metastasis, and carcinogenesis by serial analysis of gene expression. *Cancer Res* 2004; **64**: 2397–405.
11 Aung PP, Oue N, Mitani Y *et al.* Systematic search for gastric cancer-specific genes based on SAGE data: Melanoma inhibitory activity and matrix metalloproteinase-10 are novel prognostic factors in patients with gastric cancer. *Oncogene* 2006; **25**: 2546–57.
12 Sentani K, Oue N, Tashiro T *et al.* Immunohistochemical staining of Reg IV and claudin-18 is useful in the diagnosis of gastrointestinal signet ring cell carcinoma. *Am J Surg Pathol* 2008; **32**: 1182–9.
13 Hartupee JC, Zhang H, Bonaldo MF, Soares MB, Dieckgraefe BK. Isolation and characterization of a cDNA encoding a novel member of the human regenerating protein family: Reg IV. *Biochim Biophys Acta* 2001; **1518**: 287–93.
14 Oue N, Kuniyasu H, Noguchi T *et al.* Serum concentration of Reg IV in patients with colorectal cancer: Overexpression and high serum levels of Reg IV are associated with liver metastasis. *Oncology* 2007; **72**: 371–80.
15 Takehara A, Eguchi H, Ohigashi H *et al.* Novel tumor marker REG4 detected in serum of patients with resectable pancreatic cancer and feasibility for antibody therapy targeting REG4. *Cancer Sci* 2006; **97**: 1191–7.
16 Ohara S, Oue N, Matsubara A *et al.* Reg IV is an independent prognostic factor for relapse in patients with clinically localized prostate cancer. *Cancer Sci* 2008; **99**: 1570–77.
17 Sasahira T, Oue N, Kirita T *et al.* Reg IV expression is associated with cell growth and prognosis of adenoid cystic carcinoma in the salivary gland. *Histopathology* 2008; **53**: 667–75.
18 Oue N, Mitani Y, Aung PP *et al.* Expression and localization of Reg IV in human neoplastic and non-neoplastic tissues: Reg IV expression is associated with intestinal and neuroendocrine differentiation in gastric adenocarcinoma. *J Pathol* 2005; **207**: 185–98.
19 Sobin LH, Wittekind CH, eds. *TNM Classification of Malignant Tumors*, 6th edn. New York: John Wiley & Sons, 2002; 65–8.
20 Lauren P. The two histological main types of gastric carcinoma: Diffuse and so-called intestinal-type carcinoma: An attempt at a histo-clinical classification. *Acta Pathol Microbiol Scand* 1965; **64**: 31–49.
21 Sentani K, Oue N, Sakamoto N *et al.* Positive immunohistochemical staining of gammaH2AX is associated with tumor progression in gastric cancers from radiation-exposed patients. *Oncol Rep* 2008; **20**: 1131–6.
22 Schroder N, Sekhar A, Geffers I *et al.* Identification of mouse genes with highly specific expression patterns in differentiated intestinal epithelium. *Gastroenterology* 2006; **130**: 902–7.
23 Mallo GV, Rechreche H, Frigerio JM *et al.* Molecular cloning, sequencing and expression of the mRNA encoding human Cdx1 and Cdx2 homeobox. Down-regulation of Cdx1 and Cdx2 mRNA expression during colorectal carcinogenesis. *Int J Cancer* 1997; **74**: 35–44.
24 Silberg DG, Swain GP, Suh ER, Traber PG. Cdx1 and cdx2 expression during intestinal development. *Gastroenterology* 2000; **119**: 961–71.
25 Silberg DG, Sullivan J, Kang E *et al.* Cdx2 ectopic expression induces gastric intestinal metaplasia in transgenic mice. *Gastroenterology* 2002; **122**: 689–96.
26 Bai YQ, Yamamoto H, Akiyama Y *et al.* Ectopic expression of homeodomain protein CDX2 in intestinal metaplasia and carcinomas of the stomach. *Cancer Lett* 2002; **176**: 47–55.
27 Almeida R, Silva E, Santos-Silva F *et al.* Expression of intestine-specific transcription factors, CDX1 and CDX2, in intestinal metaplasia and gastric carcinomas. *J Pathol* 2003; **199**: 36–40.
28 Yamamoto H, Bai YQ, Yuasa Y. Homeodomain protein CDX2 regulates goblet-specific MUC2 gene expression. *Biochem Biophys Res Commun* 2003; **300**: 813–18.
29 Lee CS, Perreault N, Brestelli JE, Kaestner KH. Neurogenin 3 is essential for the proper specification of gastric enteroendocrine cells and the maintenance of gastric epithelial cell identity. *Genes Dev* 2002; **16**: 1488–97.
30 Bishnupuri KS, Luo Q, Murmu N, Houchen CW, Anant S, Dieckgraefe BK. Reg IV activates the epidermal growth factor receptor/Akt/AP-1 signaling pathway in colon adenocarcinomas. *Gastroenterology* 2006; **130**: 137–49.
31 Mitani Y, Oue N, Matsumura S *et al.* Reg IV is a serum biomarker for gastric cancer patients and predicts response to 5-fluorouracil-based chemotherapy. *Oncogene* 2007; **26**: 4383–93.
32 Miyazaki Y, Shinomura Y, Tsutsui S *et al.* Gastrin induces heparin-binding epidermal growth factor-like growth factor in rat gastric epithelial cells transfected with gastrin receptor. *Gastroenterology* 1999; **116**: 78–89.
33 Sugano K, Park J, Soll AH, Yamada T. Stimulation of gastrin release by bombesin and canine gastrin-releasing peptides. Studies with isolated canine G cells in primary culture. *J Clin Invest* 1987; **79**: 935–42.
34 Watson SA, Grabowska AM, El-Zaatari M, Takhar A. Gastrin—active participant or bystander in gastric carcinogenesis? *Nat Rev Cancer* 2006; **6**: 936–46.
35 Guo YS, Townsend CM, Jr. Roles of gastrointestinal hormones in pancreatic cancer. *J Hepatobiliary Pancreat Surg* 2000; **7**: 276–85.
36 Podolsky DK. Regulation of intestinal epithelial proliferation: A few answers, many questions. *Am J Physiol* 1993; **264**: 179–86.

Olfactomedin 4 (GW112, hGC-1) is an independent prognostic marker for survival in patients with colorectal cancer

NAOTSUGU SEKO[1], NAOHIDE OUE[1], TSUYOSHI NOGUCHI[3], KAZUHIRO SENTANI[1], NAOYA SAKAMOTO[1], TAKAO HINOI[2], MASAZUMI OKAJIMA[2] and WATARU YASUI[1]

Departments of [1]Molecular Pathology, and [2]Endoscopic Surgery and Surgical Science, Graduate School of Biomedical Sciences, Hiroshima University, Hiroshima; [3]Department of Gastrointestinal Surgery, Oita University Faculty of Medicine, Oita, Japan

Received August 28, 2009; Accepted October 26, 2009

DOI: 10.3892/etm_00000013

Abstract. Colorectal cancer (CRC) is one of the leading causes of cancer-related deaths worldwide. We previously performed Serial Analysis of Gene Expression (SAGE) on four primary gastric cancer samples and identified several gastric cancer-specific genes. Of these genes, *olfactomedin 4* (*OLFM4*, also known as GW112 or hGC-1) is a candidate gene for cancer-specific expression. In the present study, we examined the expression and distribution of olfactomedin 4 in CRC by immunohistochemistry. Of the 176 CRC cases, 59 (34%) were positive for cytoplasmic staining of olfactomedin 4. Olfactomedin 4-positive CRC cases showed earlier T classification (P=0.0180), N classification (P=0.0149) and stage (P=0.0144) than olfactomedin 4-negative CRC cases. In the 176 CRC patients, those with olfactomedin 4-positive CRC had a better survival rate than patients with olfactomedin 4-negative CRC (P=0.0092). Multivariate analysis indicated that T classification, M classification and negative olfactomedin 4 expression were independent predictors of survival in patients with CRC. In addition to cytoplasmic staining of olfactomedin 4, stromal staining at the invasive front was observed. In total, 29 (16%) of the 176 CRC cases were positive for stromal olfactomedin 4; however, stromal olfactomedin 4 staining was not correlated with any clinicopathologic characteristic or with patient survival. These results indicate that olfactomedin 4 is a valuable marker for long-term survival in patients with CRC.

Introduction

Colorectal cancer (CRC) is one of the leading causes of cancer-related death worldwide. An assessment of prognosis based on features of the resected tumor would permit treating physicians to qualify the benefit of adjuvant chemotherapy to individual patients. Currently, anatomic and pathologic staging is still the most accurate predictor of patient outcome. It would be valuable to supplement standard clinical and pathologic staging using molecular markers to more precisely define the subset of patients at highest or lowest risk of relapse following CRC surgery. This would facilitate better selection of patients who would benefit most from adjuvant therapy. One of the most promising molecular markers is the presence of tumor microsatellite instability (1). We previously reported that expression of Reg IV and h-prune are prognostic makers for CRC (2,3); however, these markers cannot completely identify which patients are at low or high risk for disease recurrence. Therefore, identification of better prognostic markers for patients with CRC is important.

We previously performed Serial Analysis of Gene Expression (SAGE) on four primary gastric cancer samples (4) and identified several gastric cancer-specific genes (5). Of these genes, *olfactomedin 4* (*OLFM4*, also known as GW112 or hGC-1) is a candidate gene for cancer-specific expression, at least in patients with gastric cancer. *OLFM4* was originally cloned from human hematopoietic myeloid cells (6). Although *OLFM4* is predominantly expressed in bone marrow, the small intestine, colon and prostate (6), levels of expression are much lower in normal tissues than in gastric cancer tissues (5). Enhanced olfactomedin 4 expression has been reported in gastric cancer by Northern blot analysis (7) and by immunostaining (8). Our previous immunohistochemical analysis revealed that olfactomedin 4 is expressed in 56% of gastric cancer tissues (9). In addition, olfactomedin 4 is a secreted protein, and we showed that serum olfactomedin 4 represents a novel biomarker for gastric cancer (9). In CRC patients, preoperative serum levels of olfactomedin 4 were increased in a small number of samples, and the sensitivities of serum olfactomedin 4 at stage I-III were lower than those of CEA (9).

In addition to gastric cancer, *OLFM4* mRNA and olfactomedin 4 protein overexpression have been reported in CRC (10,11). Olfactomedin 4 inhibits apoptosis and may have significant roles in the development of cancer (7). It has been proposed that olfactomedin 4 can serve as a useful marker for stem cells in the human small intestine and colon (12). In

Correspondence to: Dr Wataru Yasui, Department of Molecular Pathology, Hiroshima University Graduate School of Biomedical Sciences, 1-2-3 Kasumi, Minami-ku, Hiroshima 734-8551, Japan
E-mail: wyasui@hiroshima-u.ac.jp

Key words: olfactomedin 4, *OLFM4*, colorectal cancer, prognosis

contrast to these observations, immunohistochemical analysis has demonstrated that olfactomedin 4 down-regulation is found in late stage CRC cases and in CRC patients with shorter survival (13). The morphology and actin distribution of the HT-29 CRC cell line was altered by forced expression of olfactomedin 4. Forced expression of olfactomedin 4 did not change cell proliferation, but decreased cell adhesion and migration (13). Our previous immunohistochemical analysis in gastric cancer revealed that patients with olfactomedin 4-positive gastric cancer had a better survival rate than patients with olfactomedin 4-negative gastric cancer. These results suggest that olfactomedin 4 can inhibit tumor progression. Thus, the clinical significance of olfactomedin 4 expression in human cancers is controversial and still unclear.

Although immunohistochemical analysis of olfactomedin 4 has been performed in CRC (13), this study was performed using tissue microarray. Therefore, detailed expression and distribution of olfactomedin 4 in CRC has not yet been investigated. In the present study, we examined the expression and distribution of olfactomedin 4 in CRC by immunohistochemistry and the relationship between olfactomedin 4 staining and clinicopathologic characteristics.

Materials and methods

Tissue samples. In a retrospective study design, 176 primary tumors were collected from patients diagnosed with CRC who underwent surgery at Hiroshima University Hospital (Hiroshima, Japan). All patients underwent curative resection. Only patients without preoperative radiotherapy or chemotherapy were enrolled in the study. The patients were comprised of 105 men and 71 women. The mean age was 63 years (range, 29-89 years). Postoperative follow-up was scheduled every 1, 2 or 3 months during the first 2 years after surgery and every 6 months thereafter, unless more frequent follow-up was deemed necessary. Chest X-rays, chest computed tomography scans and serum chemistries were performed at every follow-up visit. Recurrence was evaluated from records at Hiroshima University Hospital. For immunohistochemical analysis, we used archival formalin-fixed, paraffin-embedded tissues. Histologic classification was based on the World Health Organization system. Tumor staging was performed according to the TNM stage grouping system (14). Since written informed consent was not obtained, for strict privacy protection, identifying information for all samples was removed before analysis; this procedure is in accordance with the Ethical Guidelines for Human Genome/Gene Research enacted by the Japanese Government.

Immunohistochemistry. From each patient, one or two representative tumor blocks, including the tumor center, invading front and tumor-associated non-neoplastic mucosa, were examined by immunohistochemistry. In cases of large, late-stage tumors, two different sections were examined to include representative areas of the tumor center as well as of the lateral and deep tumor invasive front. Olfactomedin 4 was detected immunohistochemically with a monoclonal antibody raised in our laboratory (9). The specificity of the anti-olfactomedin 4 antibody has been characterized in detail (9). A Dako Envision+ Mouse Peroxidase Detection System (Dako Cytomation, Carpinteria, CA, USA) was used for immunohistochemical analysis as described previously (9). In brief, antigen retrieval was carried out by microwave heating in citrate buffer (pH 6.0) for 30 min. After peroxidase activity was blocked with 3% H_2O_2-methanol for 10 min, sections were incubated with normal goat serum (Dako Cytomation) for 20 min to block nonspecific antibody binding sites. Sections were incubated with primary antibody against olfactomedin 4 (1:50) for 1 h at room temperature, followed by incubations with Envision+ anti-mouse peroxidase for 1 h. Staining was completed with a 10-min incubation with the substrate-chromogen solution. Sections were counterstained with 0.1% hematoxylin. Negative controls were created by omission of the primary antibody.

Statistical methods. Correlations between clinicopathologic parameters and olfactomedin 4 expression were analyzed by the Chi-square test. Kaplan-Meier survival curves were constructed for olfactomedin 4-positive and olfactomedin 4-negative patients. Survival rates were compared between olfactomedin 4-positive and olfactomedin 4-negative groups. Differences between survival curves were tested for statistical significance by the log-rank test (15). The Cox proportional hazards multivariate model was used to examine the association of clinical and pathologic factors and the expression of olfactomedin 4 with survival. A P-value of <0.05 was considered statistically significant.

Results

Expression and distribution of olfactomedin 4 in CRC and peritumoral mucosa. We performed immunohistochemical analysis of olfactomedin 4 in 176 human CRC samples. In CRC tissue, olfactomedin 4 staining was frequently observed in well-differentiated (Fig. 1A) and moderately differentiated adenocarcinoma (Fig. 1B). In general, staining for olfactomedin 4 was detected in the cytoplasm of tumor cells. The percentage of olfactomedin 4-stained tumor cells ranged from 0 to 80%. It has been reported that a loss/reduction in olfactomedin 4 expression at the front of the invasion is observed in CRC (13); however, the tendency for loss of olfactomedin 4 expression at the invasive front was not observed. In our previous immunohistochemical analysis of gastric cancer (9), in addition to cytoplasmic staining, extracellular staining of olfactomedin 4 was observed. In CRC tissues, extracellular staining of olfactomedin 4 was also observed. Extracellular staining of olfactomedin 4 was focal, and in general, extracellular staining of olfactomedin 4 was observed at the invasive front (Fig. 1C). The immunoreactivity for olfactomedin 4 was irregular and fibrous around tumor cells scattered in the stroma (Fig. 1D).

We then focused on the peritumoral mucosa of CRC. Notably, strong and extensive olfactomedin 4 staining was detected, and all peritumoral mucosa samples in the 176 CRC cases were positive for olfactomedin 4 regardless of the olfactomedin 4 staining in tumor cells. Olfactomedin 4 staining decreased gradually, moving away from the CRC tissue. In the mucosa closest to the tumor tissue, almost all epithelial cells showed olfactomedin 4 staining (Fig. 1E). In contrast, in the mucosa distant from the tumor tissue, few epithelial cells

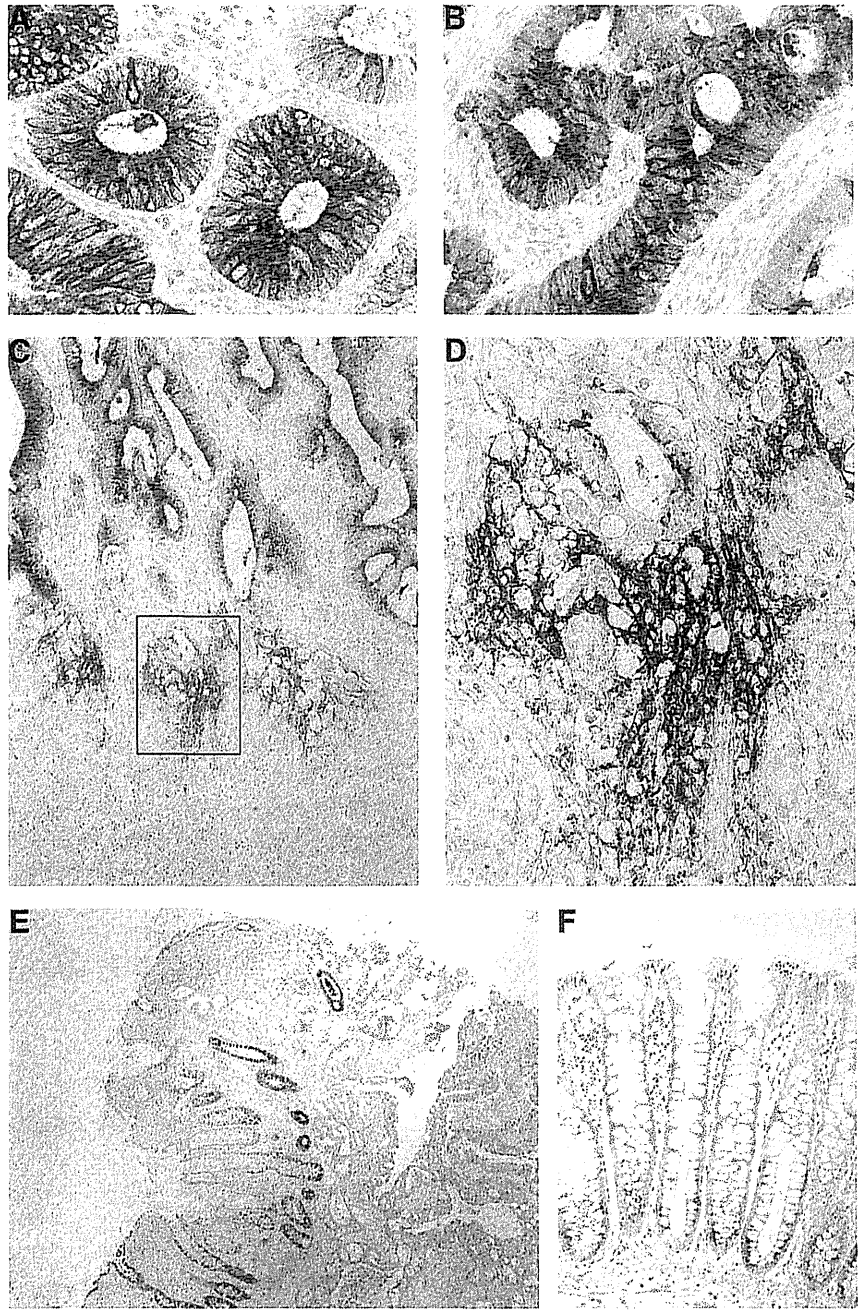

Figure 1. Immunohistochemical analysis of olfactomedin 4 in CRC and peritumoral mucosa. (A) Immunostaining of olfactomedin 4 in well-differentiated CRC. Staining of olfactomedin 4 was detected in the cytoplasm of tumor cells. Original magnification x400. (B) Immunostaining of olfactomedin 4 in moderately differentiated CRC. Staining of olfactomedin 4 was detected in the cytoplasm of tumor cells. Original magnification x400. (C) Immunostaining of olfactomedin 4 in CRC. Extracellular staining of olfactomedin 4 was observed at the invasive front. Original magnification x100. (D) High-magnification image of the field indicated by the box in C. The immunoreactivity for olfactomedin 4 was irregular and fibrous around tumor cells scattered in the stroma. Original magnification x400. (E) Immunostaining of olfactomedin 4 in the peritumoral mucosa of CRC. Almost all epithelial cells showed olfactomedin 4 staining. Original magnification x40. (F) Immunostaining of olfactomedin 4 in the mucosa distant from the tumor tissue. Few epithelial cells showed olfactomedin 4 staining. Original magnification x200.

showed olfactomedin 4 staining (Fig. 1F). Olfactomedin 4 was expressed in the basal crypt epithelium in the colon.

Relationship between olfactomedin 4 staining and clinicopathologic characteristics. The relationship of olfactomedin 4 staining with clinicopathologic characteristics was investigated (Table I). The level of olfactomedin 4 immunoreactivity was first evaluated in tumor cells. When >10% of tumor cells were stained, the immunostaining was considered positive for olfactomedin 4. In total, 59 (34%) of the 176 CRC cases were positive for olfactomedin 4. Olfactomedin 4-positive CRC cases showed earlier T classification (P=0.0180), N classification (P=0.0149) and stage (P=0.0144, all by the Chi-square test) than olfactomedin 4-negative CRC cases (Table I). Olfactomedin 4 staining was not correlated with age, gender, tumor location, M classification, or histologic classification. We also examined the relation between survival and olfactomedin 4 staining in CRC. In the 176

Table I. Correlation of olfactomedin 4 expression with clinicopathologic characteristics of 176 CRC cases.

	Olfactomedin 4 expression		
	Positive	Negative	P-value[a]
Age			0.9551
≤65	31 (33%)	62	
>65	28 (34%)	55	
Gender			0.7943
Male	36 (34%)	69	
Female	23 (32%)	48	
Tumor location			0.8075
Right/transverse	12 (35%)	22	
Left/sigmoid/rectum	47 (33%)	95	
T classification			0.0180
T1	14 (47%)	16	
T2	15 (39%)	23	
T3	24 (31%)	54	
T4	6 (20%)	24	
N classification			0.0149
N0	43 (41%)	63	
N1	16 (23%)	54	
M classification			0.6085
M0	53 (34%)	102	
M1	6 (29%)	15	
Stage			0.0144
I	26 (46%)	31	
II	16 (36%)	29	
III	11 (21%)	42	
IV	6 (29%)	15	
Histological classification			0.1973
Well/moderately	58 (35%)	110	
Poorly/mucinous	1 (13%)	7	

[a]Chi-square test.

CRC patients, those with olfactomedin 4-positive CRC had a better survival rate than patients with olfactomedin 4-negative CRC (P=0.0092, log-rank test) (Fig. 2A). It is well known that patients with CRC at stage I have a favorable rate of survival, whereas patients with CRC at stage IV show a poor rate of survival. However, it is difficult to predict the survival of patients with stage II or stage III CRC. Therefore, we analyzed the prognostic value of olfactomedin 4 in patients with stage II and III CRC. In stage II and III CRC patients (n=98), those with olfactomedin 4-positive CRC had a better survival rate than patients with olfactomedin 4-negative CRC (P=0.0347, log-rank test) (Fig. 2B). We then used Cox proportional hazards multivariate model to examine the association of clinicopathologic factors and expression of olfactomedin 4 with survival. Multivariate analysis indicated that T classification, M classification and olfactomedin 4 expression were independent predictors of survival in patients with CRC (Table II).

The level of olfactomedin 4 immunoreactivity was also evaluated in the tumor-associated stroma. Since extracellular staining of olfactomedin 4 at the invasive front was frequently observed, stromal olfactomedin 4 staining was considered positive when extracellular staining of olfactomedin 4 was stained at the invasive front. In total, 29 (16%) of the 176 CRC cases were positive for stromal olfactomedin 4. Stromal olfactomedin 4 staining was not correlated with age, gender, tumor location, T classification, N classification, M classification, stage, or histologic classification (data not shown). In the 176 CRC patients, survival rate was not statistically different between patients with stromal olfactomedin 4-positive CRC and those with stromal olfactomedin 4-negative CRC (data not shown).

Discussion

Previously, we performed SAGE on four primary gastric cancers (4) and identified several gastric cancer-specific genes (5). Of these genes, olfactomedin 4 is a candidate gene for cancer-specific expression. In the present study, we examined the expression and distribution of olfactomedin 4 in CRC by immunohistochemistry and the relationship between

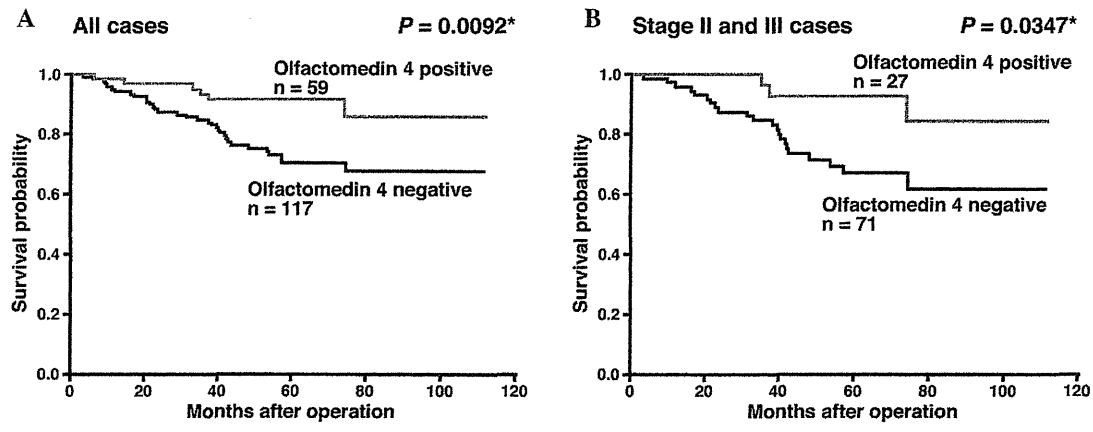

Figure 2. Survival of patients with CRC. (A) Kaplan-Meier curves of the CRC patients (all stages) with olfactomedin 4-negative or olfactomedin 4-positive tumors. (B) Kaplan-Meier curves of stage II and stage III CRC patients with olfactomedin 4-negative and olfactomedin 4-positive tumors. *Log-rank test.

Table II. Multivariate analysis of factors that influence survival of patients with CRC.

Factor	Hazard ratio	(95% CI)	Chi-square test	P-value[a]
Age			1.586	0.2078
≤65	1	(Reference)		
>65	1.511	(0.795-2.871)		
Gender			0.708	0.4001
Male	1	(Reference)		
Female	0.748	(0.381-1.470)		
Tumor location			0.368	0.5441
Right/transverse	1	(Reference)		
Left/sigmoid/rectum	0.745	(0.287-1.931)		
T classification			5.995	0.0143
T1/2	1	(Reference)		
T3/4	4.803	(1.367-16.869)		
N classification			3.488	0.0618
N0	1	(Reference)		
N1	7.327	(0.906-59.248)		
M classification			11.161	0.0008
M0	1	(Reference)		
M1	3.631	(1.704-7.737)		
Stage			1.032	0.3097
I/II	1	(Reference)		
III/IV	3.254	(0.334-31.713)		
Histologic classification			0.002	0.9632
Well/moderately differentiated	1	(Reference)		
Poorly differentiated /mucinous	0.936	(0.194-4.773)		
Olfactomedin 4 expression			4.486	0.0342
Positive	1	(Reference)		
Negative	2.725	(1.078-6.890)		

CI, Confidence interval. [a]Cox proportional hazards model.

olfactomedin 4 staining and clinicopathologic characteristics. Although few epithelial cells in colonic mucosa distant from the CRC tissue showed olfactomedin 4 staining, strong and extensive olfactomedin 4 staining was found in 34% cases of CRC, and olfactomedin 4-positive CRC cases showed earlier T classification, N classification and stage than olfactomedin 4-negative CRC cases. These results are consistent with results reported previously that olfactomedin 4 expression is up-regulated in early stage CRC and down-regulated in advanced stage CRC (13). In our previous study in gastric cancer, olfactomedin 4-positive cases were found frequently in early stage cases (9). Taken together, expression of olfactomedin 4 is an early event, and loss/reduction of olfactomedin 4 expression is a late event in gastrointestinal malignancies.

It is generally accepted that apoptosis suppresses oncogenic transformation. The ability of tumor cell populations to expand in number is determined, not only by the rate of cell proliferation, but also by the rate of cell attrition. Apoptosis represents a major source of this attrition (16). Thus, resistance to apoptosis is a hallmark of most and perhaps all types of cancer. It has been reported that olfactomedin 4 interacts with GRIM-19 to attenuate retinoic acid and interferon β-mediated cellular apoptosis, and transient expression of olfactomedin 4 promoted tumor growth in C57/BL/6 mice (7). Therefore, expression of olfactomedin 4 may contribute to carcinogenesis by resistance to apoptosis at least in early stage CRC. In contrast, forced expression of olfactomedin 4 in an HT-29 cell line decreased cell adhesion and migration (13). Therefore, it is possible that loss/reduction of olfactomedin 4 expression induces tumor cell invasion in late stage CRC cases.

In the present study, univariate and multivariate analyses revealed that negative expression of olfactomedin 4 is a prognostic indicator. Furthermore, negative expression of olfactomedin 4 correlated with a short survival rate in stage II and III CRC cases. Patients diagnosed with stage II or III CRC have variable prognoses, and they are the group that would benefit most from discovery of a prognostic factor that can identify individuals for whom adjuvant treatment would be most advantageous. To clarify whether olfactomedin 4 immunostaining is useful for identification of patients most likely to benefit from adjuvant treatment, association between

olfactomedin 4 staining and response to adjuvant therapies should be investigated.

In addition to cytoplasmic olfactomedin 4 staining, extracellular staining was also observed. Extracellular staining of olfactomedin 4 at the invasive front was frequently observed. Observation of the invasive front is important in the analysis of tumor cells, since it reflects the invasive potential of tumor cells. It has been reported that the expression of matrilysin in the invasive front is a promising biomarker predicting nodal metastasis of CRC (17). Overexpression of heparanase at the invasive front has been reported in gastric cancer and high expression of heparanase was a strong predictor of poor survival (18). These results indicate that the proteolytic degradation of the extracellular matrix by these molecules is one of the most important mechanisms in tumor progression, and the proteolytic degradation occurs at the invasive front. Although there was no correlation between stromal expression of olfactomedin 4 and clinicopathologic characteristics, stromal expression of olfactomedin 4 at the invasive front may partly contribute to the malignant behavior of CRC, such as local invasiveness.

Notably, extensive olfactomedin 4 staining was observed in the peritumoral mucosa of CRC, and olfactomedin 4 staining decreased gradually, moving away from the tumor tissue. It is well known that the peritumoral mucosa of CRC is often hyperplastic, and various growth factors, such as transforming growth factor-α and basic fibroblast growth factor, are increased in the peritumoral mucosa (19). Since expression of olfactomedin 4 in the crypt epithelium of inflamed colonic mucosa has been reported (20), olfactomedin 4 expression may be induced by growth factors and may function as an antiapoptotic factor in the peritumoral mucosa of CRC.

In summary, we showed that olfactomedin 4 is a valuable marker for long survival in patients with CRC. However, the significance of extracellular staining of olfactomedin 4 at the invasive front and extensive olfactomedin 4 staining in the peritumoral mucosa of CRC remains unclear. Since olfactomedin 4 is a secreted protein, identification of a cell surface receptor for olfactomedin 4 will further improve our understanding of the basic biology of olfactomedin 4.

Acknowledgements

We thank Mr Shinichi Norimura for the excellent technical assistance and advice. We thank the Analysis Center of Life Science, Hiroshima University for the use of their facilities. This work was supported, in part, by Grants-in-Aid for Cancer Research from the Ministry of Education, Culture, Science, Sports and Technology of Japan, in part, by a Grant-in-Aid for the Third Comprehensive 10-Year Strategy for Cancer Control and for Cancer Research from the Ministry of Health, Labour and Welfare of Japan and in part by a grant (07-23911) from the Princess Takamatsu Cancer Research Fund.

References

1. Popat S, Hubner R and Houlston RS: Systematic review of microsatellite instability and colorectal cancer prognosis. J Clin Oncol 23: 609-618, 2005.
2. Oue N, Kuniyasu H, Noguchi T, *et al*: Serum concentration of Reg IV in patients with colorectal cancer: overexpression and high serum levels of Reg IV are associated with liver metastasis. Oncology 72: 371-380, 2007.
3. Kobayashi T, Hino S, Oue N, Asahara T, Zollo M, Yasui W and Kikuchi A: Glycogen synthase kinase 3 and h-prune regulate cell migration by modulating focal adhesions. Mol Cell Biol 26: 898-911, 2006.
4. Oue N, Hamai Y, Mitani Y, *et al*: Gene expression profile of gastric carcinoma: identification of genes and tags potentially involved in invasion, metastasis and carcinogenesis by serial analysis of gene expression. Cancer Res 64: 2397-2405, 2004.
5. Aung PP, Oue N, Mitani Y, *et al*: Systematic search for gastric cancer-specific genes based on SAGE data: melanoma inhibitory activity and matrix metalloproteinase-10 are novel prognostic factors in patients with gastric cancer. Oncogene 25: 2546-2557, 2006.
6. Zhang J, Liu WL, Tang DC, *et al*: Identification and characterization of a novel member of olfactomedin-related protein family, hGC-1, expressed during myeloid lineage development. Gene 283: 83-93, 2002.
7. Zhang X, Huang Q, Yang Z, Li Y and Li CY: GW112, a novel antiapoptotic protein that promotes tumor growth. Cancer Res 64: 2474-2481, 2004.
8. Liu W, Zhu J, Cao L and Rodgers GP: Expression of hGC-1 is correlated with differentiation of gastric carcinoma. Histopathology 51: 157-165, 2007.
9. Oue N, Sentani K, Noguchi T, *et al*: Serum olfactomedin 4 (GW112, hGC-1) in combination with Reg IV is a highly sensitive biomarker for gastric cancer patients. Int J Cancer 125: 2383-2392, 2009.
10. Koshida S, Kobayashi D, Moriai R, Tsuji N and Watanabe N: Specific overexpression of OLFM4 (GW112/HGC-1) mRNA in colon, breast and lung cancer tissues detected using quantitative analysis. Cancer Sci 98: 315-320, 2007.
11. Conrotto P, Roesli C, Rybak J, *et al*: Identification of new accessible tumor antigens in human colon cancer by ex vivo protein biotinylation and comparative mass spectrometry analysis. Int J Cancer 123: 2856-2864, 2008.
12. Van der Flier LG, Haegebarth A, Stange DE, van de Wetering M and Clevers H: OLFM4 is a robust marker for stem cells in human intestine and marks a subset of colorectal cancer cells. Gastroenterology 137: 15-17, 2009.
13. Liu W, Liu Y, Zhu J, Wright E, Ding I and Rodgers GP: Reduced hGC-1 protein expression is associated with malignant progression of colon carcinoma. Clin Cancer Res 14: 1041-1049, 2008.
14. Sobin LH and Wittekind CH (eds): TNM Classification of Malignant Tumors. 6th edition. Wiley-Liss, New York, pp65-68, 2002.
15. Mantel N: Evaluation of survival data and two new rank order statistics arising in its consideration. Cancer Chemother Rep 50: 163-170, 1966.
16. Hanahan D and Weinberg RA: The hallmarks of cancer. Cell 100: 57-70, 2000.
17. Kurokawa S, Arimura Y, Yamamoto H, *et al*: Tumour matrilysin expression predicts metastatic potential of stage I (pT1) colon and rectal cancers. Gut 54: 1751-1758, 2005.
18. Takaoka M, Naomoto Y, Ohkawa T, *et al*: Heparanase expression correlates with invasion and poor prognosis in gastric cancers. Lab Invest 83: 613-622, 2003.
19. Kuniyasu H, Yasui W, Shinohara H, *et al*: Induction of angiogenesis by hyperplastic colonic mucosa adjacent to colon cancer. Am J Pathol 157: 1523-1535, 2000.
20. Shinozaki S, Nakamura T, Iimura M, *et al*: Upregulation of Reg 1 alpha and GW112 in the epithelium of inflamed colonic mucosa. Gut 48: 623-629, 2001.

The American Journal of Pathology, Vol. 176, No. 4, April 2010

DOI: 10.2353/ajpath.2010.090500

Cell Injury, Repair, Aging and Apoptosis

Role of Insulin-Like Growth Factor Binding Protein 2 in Lung Adenocarcinoma

IGF-Independent Antiapoptotic Effect Via Caspase-3

Toshiro Migita,* Tadahito Narita,*† Reimi Asaka,* Erika Miyagi,* Hiroko Nagano,* Kimie Nomura,* Masaaki Matsuura,‡§ Yukitoshi Satoh,¶ Sakae Okumura,¶ Ken Nakagawa,¶ Hiroyuki Seimiya,‖ and Yuichi Ishikawa*

From the Divisions of Pathology, and Cancer Genomics,‡ The Cancer Institute, Tokyo; Zenyaku Kogyo Co., Ltd.,† Tokyo; the Bioinformatics Group,§ Genome Center, Tokyo; the Department of Thoracic Surgical Oncology,¶ and the Division of Molecular Biotherapy,‖ Cancer Chemotherapy Center, The Cancer Institute Hospital, Japanese Foundation for Cancer Research, Tokyo, Japan*

Insulin-like growth factor (IGF) signaling plays a pivotal role in cell proliferation and mitogenesis. Secreted IGF-binding proteins (IGFBPs) are important modulators of IGF bioavailability; however, their intracellular functions remain elusive. We sought to assess the antiapoptotic properties of intracellular IGFBP-2 in lung adenocarcinomas. IGFBP-2 overexpression resulted in a decrease in procaspase-3 expression; however, it did not influence the phosphorylation status of either IGF receptor or its downstream targets, including Akt and extracellular signal-regulated kinase. Apoptosis induced by camptothecin was significantly inhibited by IGFBP-2 overexpression in NCI-H522 cells. Conversely, selective knockdown of IGFBP-2 using small-interfering RNA resulted in an increase in procaspase-3 expression and sensitization to camptothecin-induced apoptosis in NCI-H522 cells. LY294002, an inhibitor of phosphatidylinositol 3-kinase, caused a decrease in IGFBP-2 levels and enhanced apoptosis in combination with camptothecin. Immunohistochemistry demonstrated that intracellular IGFBP-2 was highly expressed in lung adenocarcinomas compared with normal epithelium. Intracellular IGFBP-2 and procaspase-3 were expressed in a mutually exclusive manner. These findings suggest that intracellular IGFBP-2 regulates caspase-3 expression and contributes to the inhibitory effect on apoptosis independent of IGF. IGFBP-2, therefore, may offer a novel therapeutic target and serve as an antiapoptotic biomarker for lung adenocarcinoma. *(Am J Pathol 2010, 176:1756–1766; DOI: 10.2353/ajpath.2010.090500)*

Insulin-like growth factor-I and -II (IGF-I and -II) are important regulators of cellular metabolism, growth, and survival. When IGFs bind to their receptors, the type I and type II IGF receptors (IGF-IR or IGF-IIR), they activate the downstream signaling cascades via the phosphorylation of tyrosine kinase. Activated IGF-1R transmits signals to the major distinct pathways mitogen-activated protein kinase and phosphatidyl inositol 3-kinase (PI3K), signaling pathways that are highly implicated in the development and progression of neoplasia. IGF's bioavailability is regulated by six high affinity IGF binding proteins (IGFBPs). Secreted IGFBPs by cancer cells interfere primarily with IGF-I or -II through the formation of IGF-IGFBPs complex, which in turn exert an inhibitory effect on IGF-mediated biological functions.

IGF-independent functions of extracellular IGFBPs have long been discussed. Secreted and membrane-associated IGFBP-2 directly binds to proteoglycans and integrins,[1–5] demonstrating IGFBP-2 as a negative or positive regulator of cell adhesion, migration, and invasion in an IGF-independent manner. In the same way, IGFBP-2 positively or negatively regulates cell growth

Supported by Grants-in-Aid for Scientific Research on Priority Areas from the Ministry of Education, Culture, Sports, Science, and Technology; Grants-in-Aid for Scientific Research from the Japan Society for the Promotion of Science; and by grants from the Ministry of Health, Labor, and Welfare, the National Institute of Biomedical Innovation, the Smoking Research Foundation, and the Vehicle Racing Commemorative Foundation.

Accepted for publication December 8, 2009.

Current address of T.M., Division of Molecular Biotherapy, Cancer Chemotherapy Center, Japanese Foundation for Cancer Research, Tokyo, Japan.

Address reprint requests to Toshiro Migita, M.D., Ph.D., Division of Molecular Biotherapy, Cancer Chemotherapy Center, Japanese Foundation for Cancer Research, 3-8-31, Ariake, Koto-ku, Tokyo 135-8550, Japan. E-mail: toshiro.migita@jfcr.or.jp.

and survival in certain types of cancers *in vitro*.[2,6–11] In *in vivo* studies, the growth of mice colorectal adenomas induced by chemical carcinogen was inhibited when they were crossed with IGFBP-2 transgenic mice[12]; however, in contrast, IGFBP-2 exerts oncogenic effects in brain-specific transgenic mice.[13] Thus, increased IGFBP-2 confers advantage or disadvantage for tumor growth, depending on cell type and physiological conditions.[2,14]

Despite these two opposite effects of IGFBP-2 on biological behaviors of cancers, biochemistry and molecular pathology have demonstrated that IGFBP-2 is overexpressed in a wide variety of human malignancies, including glioma,[15] prostate cancer,[16] lung cancer,[17–19] colorectal cancer,[20] ovarian cancer,[21] adrenocortical tumor,[22] breast cancer,[23] and leukemia.[24] Importantly, IGFBP-2 is frequently overexpressed in advanced cancers and is suggested to be involved in the metastatic process.[25] Several potential mechanisms of cancer progression mediated by secreted IGFBP-2 are discussed,[14] but little study has been conducted to the analysis of intracellular-IGFBP-2 functions.

Our aim for this study is to examine the effect of intracellular IGFBP-2 on apoptosis in lung cancer cells and elucidate its molecular mechanism. We also examine the significance of intracellular IGFBP-2 and procaspase-3 in clinical samples and explore the therapeutic implications.

Materials and Methods

Cell Culture and Clinical Samples

The human lung adenocarcinoma cell lines A549, NCI-H460, NCI-H23, NCI-H522, HOP62, COR-L105, and PC14 were obtained from the American Type Culture Collection (Manassas, VA) and grown in RPMI 1640 media supplemented with 10% fetal bovine serum (both medium and serum were from Gibco-BRL, Tokyo, Japan) and 1% penicillin/streptomycin in an atmosphere of 5% CO_2 at 37°C, as previously described.[26]

We also analyzed the mRNA and protein expression in 24 pairs of primary lung adenocarcinomas and corresponding normal lung tissues. All experiments were performed by using a protocol approved by the Institutional Review Board of the Japanese Foundation for Cancer Research (number 2007-1058).

Transient and Stable Transfections

IGFBP-2 cDNA expression construct in pcDNA3.1/Neo (Invitrogen, Carlsbad, CA) was a generous gift from Dr. Hiroaki Kataoka (Section of Oncopathology and Regenerative Biology, Department of Pathology, University of Miyazaki, Japan).[27] Cells were plated at 7×10^5 per well in 60-mm dishes and transfected in triplicate by using the FuGENE 6 Transfection Reagent according to the manufacturer's protocol (Roche Diagnostics, Inc., Indianapolis, IN). We established stable cell lines COR-L105, NCI-H522, and HOP62 overexpressing IGFBP-2 after 4 weeks of selection in 400 μg/ml of neomycin.

RNA Preparation and Real-Time RT-PCR

The cells and frozen tissue were collected for RNA extraction by using an RNeasy Kit (Qiagen, Valencia, CA), and total RNA was applied for first-strand cDNA synthesis with a high capacity cDNA Reverse Transcriptase kit (Applied Biosystems, Foster City, CA). Gene-specific probes and primer were obtained from Universal Probe-Library (number 25, Roche Applied Science, Tokyo, Japan), and primer sequences were as follows: 5′-TTGCAGACAATGGCGATGACC-3′ (IGFBP-2 forward); 5′-GGGATGTGCAGGGAGTAGAGG-3′ (IGFBP-2 reverse). PCR was performed in 96-well plates by using the LightCycler 480 System (Roche Applied Science). All reactions were performed at least in triplicate. The relative amounts of all mRNAs were calculated by using the comparative threshold cycle (CT) method after normalization to human β2 microglobulin.

Cell Lysis and Immunoblotting

To obtain total protein lysates, frozen tissue and cells were homogenized and dissolved in radioimmunoprecipitation assay buffer (150 mmol/L of NaCl, 1.0% Nonidet P40, 0.5% sodium deoxycholate, 0.1% SDS, 50 mmol/L of Tris, pH 7.6) containing proteinase inhibitors and phosphatase inhibitors (Nacalai Tesque, Kyoto, Japan). The protein concentration of each lysate was determined by using a protein assay reagent kit (BioRad, Hercules, CA). The total cell lysate was applied on 4% to 12% SDS-polyacrylamide gel electrophoresis. After electrophoresis, the proteins were transferred electrophoretically from the gel to polyvinylidene difluoride membranes (Millipore, Bedford, MA). The membranes were then blocked for 1 hour in blocking buffer (5% low-fat dried milk in Tris-buffered saline) and probed with the primary antibodies overnight. After being washed, the protein content was made visible with horseradish-peroxidase-conjugated secondary antibodies followed by enhanced chemiluminescence (Amersham, Piscataway, NJ). Signal densities were quantitatively determined by ImageJ 1.36 b software (NIH, Bethesda, MD). The primary antibodies used were raised against IGFBP-2 (C-18, Santa Cruz Biotechnology, Santa Cruz, CA), caspase-3, phosphorylated (Tyr1135/1136) and total IGF-1R β, phosphorylated (Ser 473) and total Akt, phosphorylated (Thr 202/Tyr 204) and total Erk1/2, cleaved poly ADP-ribose polymerase (PARP; all obtained from Cell Signaling Technology, Danvers, MA), and β-actin (Sigma, St. Louis, MO). LY294002 was purchased from Sigma.

Caspase Activity Assay

Caspase activities were measured by using the Caspase-Glo 3/7 assay kit according to the manufacturer's instruction (Promega, Madison, WI). Cells (5×10^3 cells/well) were placed in a 96-well culture plate, followed by treatment with dimethyl sulfoxide (DMSO) vehicle or 200 nmol/L of camptothecin for 24 hours. One hundred microliters of Caspase-Glo 3/7 reagent was added to each well and incubated for 1 hour at room temperature.

The culture media with the reagent served as blank, and blank control value was subtracted from each sample value. Luminescence of all samples was measured by using a Tecan Spectrafluor Plus (Wako, Osaka, Japan).

Enzyme-Linked Immunosorbent Assay

IGFBP-2 concentrations in media of cell culture were determined with IGFBP-2 Duoset enzyme-linked immunosorbent assay (ELISA) Development system (R and D Systems, Minneapolis, MN) according to the manufacturer's protocol. Briefly, capture antibody was plated in a 96-well microplate and incubated overnight at room temperature. One hundred microliters of supernatant of culture media or IGFBP-2 standard were added into plate and incubate for 2 hours at room temperature, followed by the immunoreaction with IGFBP-2 detection antibody. IGFBP-2 concentration was calculated from the standard curve. All experiments were performed in duplicate or triplicate.

RNA Interference

Small-interfering RNA (siRNA) oligonucleotides for IGFBP-2 (Santa Cruz Biotechnology) and a negative control (Invitrogen) were transfected into the cells. Transfection was performed by using Lipofectamine RNAiMAX (Invitrogen) according to the manufacturer's protocol. Briefly, 60 pmol of siRNA and 10 μl of Lipofectamine RNAiMAX were mixed in 1 ml of Opti-MEM medium (10 nmol/L of final siRNA concentration). After 20 minutes of incubation, the mixture was added to the suspended cells and these were plated on dishes. Cells were harvested at 24-hour intervals until 72 hours after transfection.

Cell Proliferation and Apoptosis

Cell proliferation was measured as the number of viable cells, as evaluated at 450 nm optical density by using Cell Count reagent SF (Nacalai Tesque). Apoptotic cells were determined by Hoechst 33342 staining, and the apoptosis rate (percent of total population) was evaluated by counting apoptotic and nonapoptotic cells in at least three randomly selected fields.

Immunohistochemistry

Tissue microarrays were constructed from 169 paraffin-embedded lung adenocarcinomas. Briefly, H&E-stained sections containing representative tumor regions were selected. Tissues were punched from cancer areas of each donor block by using tissue cylinders with a diameter of 2 mm and then brought into a recipient paraffin block. Three tumor cores were taken per patient.

Immunohistochemistry was performed on 5-μm thick, formalin-fixed, paraffin-embedded sections by using primary antibodies for IGFBP-2 (C-18, Santa Cruz Biotechnology) and procaspase-3 (Cell Signaling Technology). Antigen retrieval was performed for 30 minutes in citrate buffer for each antibody. The slides were developed by using the labeled streptavidin biotinylated peroxidase method (Nichirei, Tokyo, Japan) according to the manufacturer's instructions. 3,3′-Diaminobenzidine tetrahydro-chloride was used as the chromogen, and hematoxylin was used as the counterstain. A549 xenografts in nude mice were previously established[26] and were used as a positive control. The primary antibody was omitted for negative controls. All immunohistochemical staining was accomplished with a Dako Autostainer (DakoCytomation, Carpenteria, CA) under the same conditions. The staining intensity of IGFBP-2 and procaspase-3 was scored semiquantitatively: positive in less than 25% of cancer cells (weak), positive in 25% to 50% of cancer cells (moderate), and positive in more than 50% of cancer cells (strong). Representative score of each patient was defined as the highest score across three cores.

Statistical Analysis

For *in vitro* experiments, statistical analysis was performed by using Welch's *t*-tests. Comparisons of IGFBP-2 mRNA levels in clinical samples were made by using paired *t*-test analysis. Dose/time dependency of drugs was determined by the confidence interval (CI) based test of slope of the linear regression. Concentrations of drugs that suppressed cell proliferation to 50% of levels exhibited by control cells (IC50) were derived from the dose-response curve. Correlation between IGFBP-2 and caspase-3 expression in immunohistochemistry was evaluated by performing the Fisher's exact test. For all analyses, $P \leq 0.05$ was considered statistically significant. Statistical analyses were performed by using the statistical programming language of R (http://www.R-project.org; accessed February 1, 2010) and Statistika (Statsoft, Inc., Tulsa, OK).

Results

IGFBP-2 Is Expressed and Secreted in Lung Adenocarcinoma Cell Lines

At first, intracellular IGFBP-2 expression levels were examined in various lung cancer cell lines by the use of Western blot. IGFBP-2 was highly expressed in A549, NCI-H460 cells, but expressed at very low levels in HOP62 and COR-L105 cells (Figure 1A).

The levels of secreted IGFBP-2 in media were measured by ELISA. Secreted IGFBP-2 levels correlated with intracellular protein levels obtained by Western blot (Figure 1B).

IGFBP-2 Expression Is Regulated Transcriptionally and Posttranslationally

IGFBP-2 expression is physiologically up-regulated by the energy restriction or insulin-dependent diabetes mellitus.[28,29] To determine whether the supplement of nutrients can alter IGFBP-2 expression in lung cancer cells, we examined the effects of glucose or serum depletion on IGFBP-2 expression in A549 cells. Glucose depletion significantly reduced IGFBP-2 levels at both protein and mRNA levels ($P = 0.0017$), whereas serum depletion did not ($P = 0.311$; Figure 2A). IGFBP-2 protein and mRNA levels were dependent on glucose concentration (Figure 2B). These findings suggest that IGFBP-2 expression in

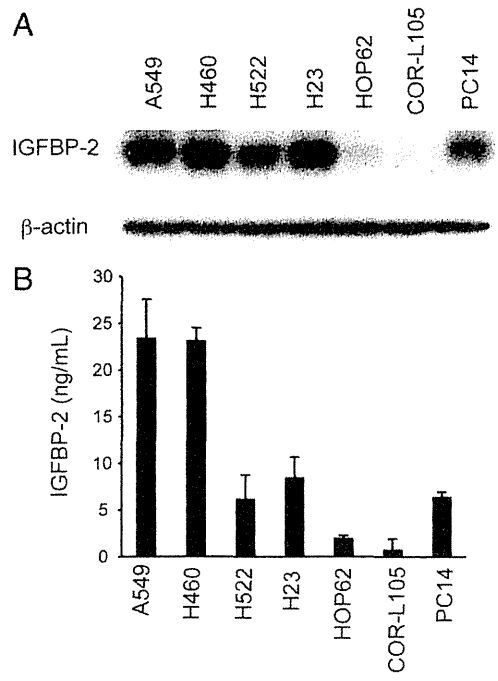

Figure 1. A: Basal levels of intracellular IGFBP-2 protein in seven lung adenocarcinoma cell lines. Cells (5×10^5) were plated in a 60-mm dish and cultured for 48 hours. The protein extracts from each cell line were resolved by SDS-polyacrylamide gel electrophoresis and blotted with an antibody against IGFBP-2. β-actin served as internal control. A representative data from two independent experiments is shown. **B:** Conditioned media containing a different amount of IGFBP-2 in lung adenocarcinoma cell lines. Secreted IGFBP-2 was measured, under the same conditions as above, by ELISA. Values represent means ± SD.

cancer cells is glucose-dependent and is regulated by a mechanism that is distinct from normal cells.

It has been reported that IGFBP-2 expression is regulated by the PI3K-PTEN (phosphatase and tensin homolog deleted on chromosome 10) pathway in prostate and glioblastoma cells.[30] Thus, extracellular and intracellular IGFBP-2 levels were evaluated in lung cancer cells treated with LY294002, a PI3K inhibitor. PTEN protein was detected in all cell lines, except PC14, as described previously.[26] Secretion of IGFBP-2 protein was suppressed in all cell lines by the treatment of LY294002 to varying degrees (Figure 2C). The effect of LY294002 on IGFBP-2 expression showed a significant dose dependence ($P = 0.0048$) and time course dependence (95% CI: 0.134 to 0.18, control; 0.029 to 0.043, LY294002) in A549 cells (Figure 2, D and E). Intracellular IGFBP-2 levels were also decreased with LY294002 (Figure 2F). Interestingly, a fraction of IGFBP-2 protein was degraded into approximately 20 kDa after treatment with LY294002 (Figure 2F). Conversely, IGFBP-2 mRNA was significantly increased with LY294002 ($P < 0.005$; Figure 2G), suggesting the existence of a compensatory feedback mechanism.

IGFBP-2 Overexpression Suppresses Procaspase-3 Expression and Confers Resistance for Drug-induced Apoptosis

To address whether IGFBP-2 is involved in apoptotic event, IGFBP-2 was enforced in cells with low endogenous IGFBP-2 levels, and then caspase expression was examined. IGFBP-2 overexpression resulted in a remarkable increase in intracellular IGFBP-2 levels in COR-L105, NCI-H522, and HOP62 cells compared with vector control (Figure 3A). Secreted IGFBP-2 levels of these cells were also increased corresponding to the levels of intracellular IGFBP-2 (Figure 3B). Intriguingly, IGFBP-2 overexpression resulted in a substantial decrease in procaspase-3 expression (Figure 3A). However, caspase-9 was not decreased (Figure 3A), suggesting IGFBP-2 specifically inhibits caspase-3 expression. Despite a higher amount of IGFBP-2 secretion into media, no significant changes were found in the IGF signaling pathway including phosphorylation statuses of IGF-1R, Akt, or Erk1/2 (Figure 3A). These findings suggest that IGFBP-2-mediated caspase-3 inhibition occurs in an IGF-independent manner.

Next, to examine whether IGFBP-2 involves in apoptotic event, we compared the sensitivity of IGFBP-2 overexpressing cells and vector control cells to an apoptosis inducer, camptothecin. IGFBP-2 overexpressing and vector control H522 cells were exposed to 20 to 1000 nmol/L of camptothecin for 24 hours, and the cell proliferation and caspase-3 activity were analyzed. The results indicated that IGFBP-2 overexpressing H522 cells were significantly resistant to camptothecin (EV, IC50 = 686 nmol/L; BP-2, IC50 > 1000 nmol/L; Figure 3C). As expected, caspase-3 activity was significantly decreased in IGFBP-2 overexpressing cells compared with vector control cells on treatment with camptothecin ($P < 0.02$; Figure 3D). Apoptosis was evaluated by Hoechst 33342 staining and PARP cleavage. Enforced IGFBP-2 significantly inhibited PARP cleavage, as determined by Western blot (Figure 3E), and reduced camptothecin-induced apoptotic cells in H522 cells ($P = 0.003$; Figure 3F). Similar results were obtained with the treatment of cisplatin or etoposide (data not shown).

IGFBP-2 Inhibition Up-Regulates Procaspase-3 Expression and Promotes Drug-Induced Apoptosis

To further elucidate the effects of IGFBP-2 on caspase-3, gene silencing for IGFBP-2 was performed in A549 and H522 cells. IGFBP-2 knockdown induced an increase in procaspase-3 expression until 72 hours after siRNA treatment in both cell lines (Figure 4A). No significant active form of cleaved caspase-3 was identified (data not shown). As is the results with IGFBP-2 overexpression, no substantial change was found in caspase-9. In addition, IGFBP-2 siRNA also decreased the phosphorylation status of IGF-1R. This effect might be because of a rapid decrease in both intracellular and extracellular IGFBP-2. Although IGFBP-2 knockdown resulted in morphological changes such as shrinkage in A549 cells, no substantial increase in apoptosis was identified by Hoechst 33342 staining or PARP cleavage (data not shown).

We now asked whether IGFBP-2 inhibition sensitizes cells for drug-induced apoptosis. Figure 4B shows the cell proliferation of IGFBP-2 knockdown and negative control cells with a treatment of camptothecin. IGFBP-2

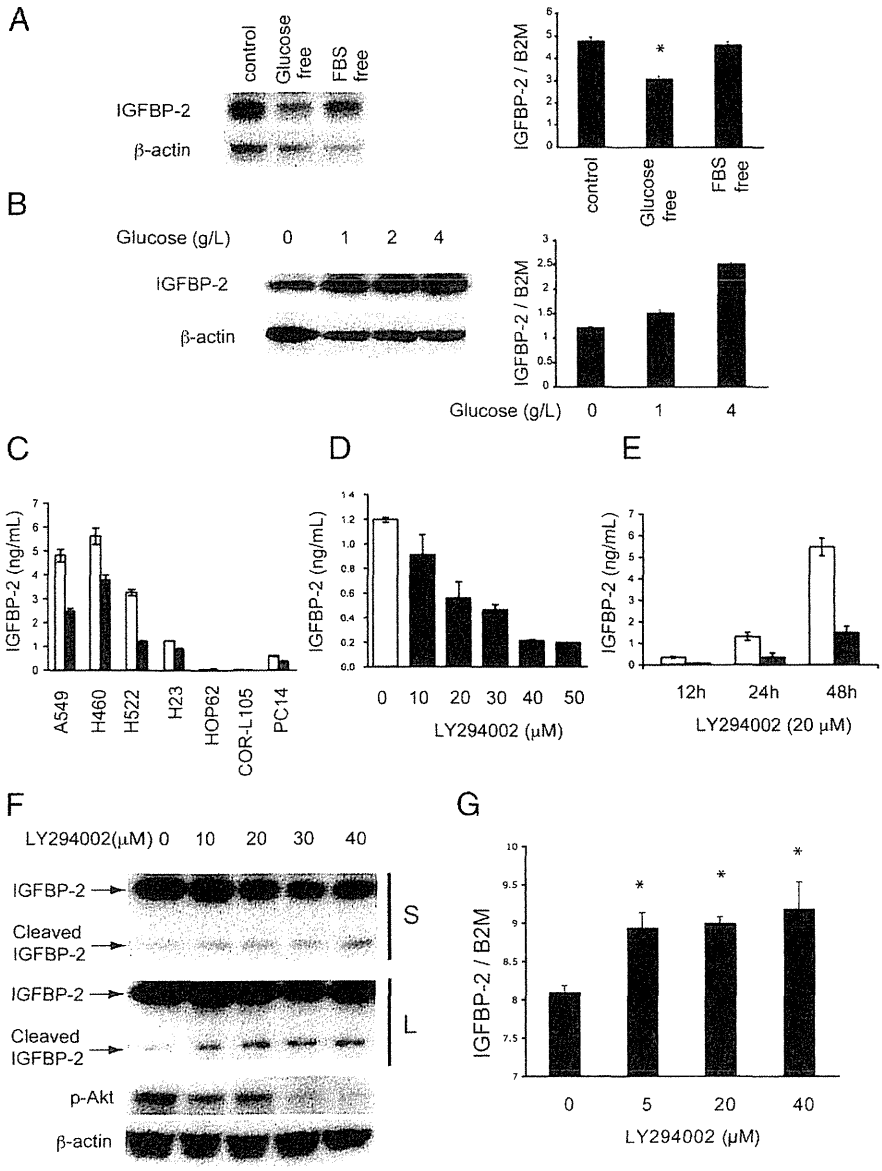

Figure 2. A: The effect of glucose and fetal bovine serum on intracellular IGFBP-2 levels. A549 cells (5×10^5) were incubated for 2 hours in fetal bovine serum (FBS) free media, followed by a 24-hour incubation in glucose free, FBS free, or regular media. The cells were then harvested and subjected to both immunoblotting and quantitative RT-PCR for IGFBP-2. IGFBP-2 mRNA was normalized to human β2 microglobulin (B2M). Values represent means ± SD. Statistical analysis was performed by Welch's *t*-test. $^*P < 0.01$. **B:** A549 cells were cultured in media with the indicated concentrations of glucose for 24 hours. IGFBP-2 expression levels were measured by both immunoblotting and quantitative RT-PCR. Values represent means ± SD. Significant slope of regression line between IGFBP-2 mRNA and glucose concentration was obtained ($P = 0.012$). **C:** Effect of LY294002, a PI3K inhibitor, on extracellular IGFBP-2 levels. Seven lung adenocarcinoma cell lines were treated either with a vehicle control DMSO (white bar) or 20 μmol/L of LY294002 (black bar) for 24 hours. Secreted IGFBP-2 was measured by ELISA as described before. **D:** A549 cells were treated with the indicated concentration of LY294002 for 24 hours. A significant slope of regression line between secreted IGFBP-2 and LY294002 concentration was obtained ($P = 0.0048$). **E:** Time course of IGFBP-2 secretion in A549 cells treated with 20 μmol/L of LY294002. The 95% CI based test of slope regression was significant ($P < 0.05$): 0.134 to 0.18 vs. 0.029 to 0.043, in control DMSO and LY294002, respectively. **F:** The effect of LY294002 on intracellular levels of IGFBP-2. A549 cells were treated with the indicated concentration of LY294002, followed by immunoblotting for IGFBP-2, phosphorylated Akt (Ser 473), and β-actin. S, short exposure; L, long exposure. **G:** A549 cells were treated with the indicated concentration of LY294002, and IGFBP-2 mRNA levels were evaluated by a real-time RT-PCR. Values represent means ± SD. Statistical analysis was performed by Welch's *t*-test. $^*P < 0.01$.

knockdown cells were more sensitive to camptothecin rather than vector control cells (95% CI: -2.7×10^{-4} to -1.6×10^{-4} vs. -4.5×10^{-4} to -3.0×10^{-4}, in negative control and IGFBP-2 siRNA, respectively; Figure 4B). In caspase-3 activity assay (Figure 4C), there were no significant changes in caspase-3 activity between negative control and IGFBP-2 siRNA with DMSO treatment (white bars). When cells were treated with camptothecin, IGFBP-2 siRNA significantly increased caspase-3 activity than negative control siRNA (black bars). The sensitivity to camptothecin was significantly potentiated by IGFBP-2 inhibition ($P < 0.0001$). Apoptosis was significantly increased in cells with IGFBP-2 siRNA compared with negative control siRNA ($P = 0.0009$; Figure 4D). Cleaved PARP was more substantial in IGFBP-2 siRNA treated cells compared with vector control H522 cells (Figure 4E). As a PI3K inhibitor induced IGFBP-2 degradation (Figure 2F), we examined whether a PI3K inhibitor has an additive effect on apoptosis with camptothecin. As expected, combination therapy of LY294002 and camptothecin enhanced PARP cleavage in H522 cells when compared with camptothecin or LY294002 alone. IGFBP-2 levels were inversely correlated with the increase in the levels of cleaved PARP (Figure 4F, left panels). In contrast, there were no substantial effects of LY294002 on PARP cleavage in COR-L105 cells, which have low IGFBP-2 levels (Figure 4F, right panels).

These data strongly suggest that IGFBP-2 regulates apoptosis via caspase-3. Moreover, IGFBP-2 becomes a therapeutic target as well as a biomarker for the treatment of PI3K inhibitors.

Tissue IGFBP-2 Is Overexpressed in Lung Adenocarcinoma

Next, we examined tissue expression levels of IGFBP-2 in human lung adenocarcinoma and normal tissue by using

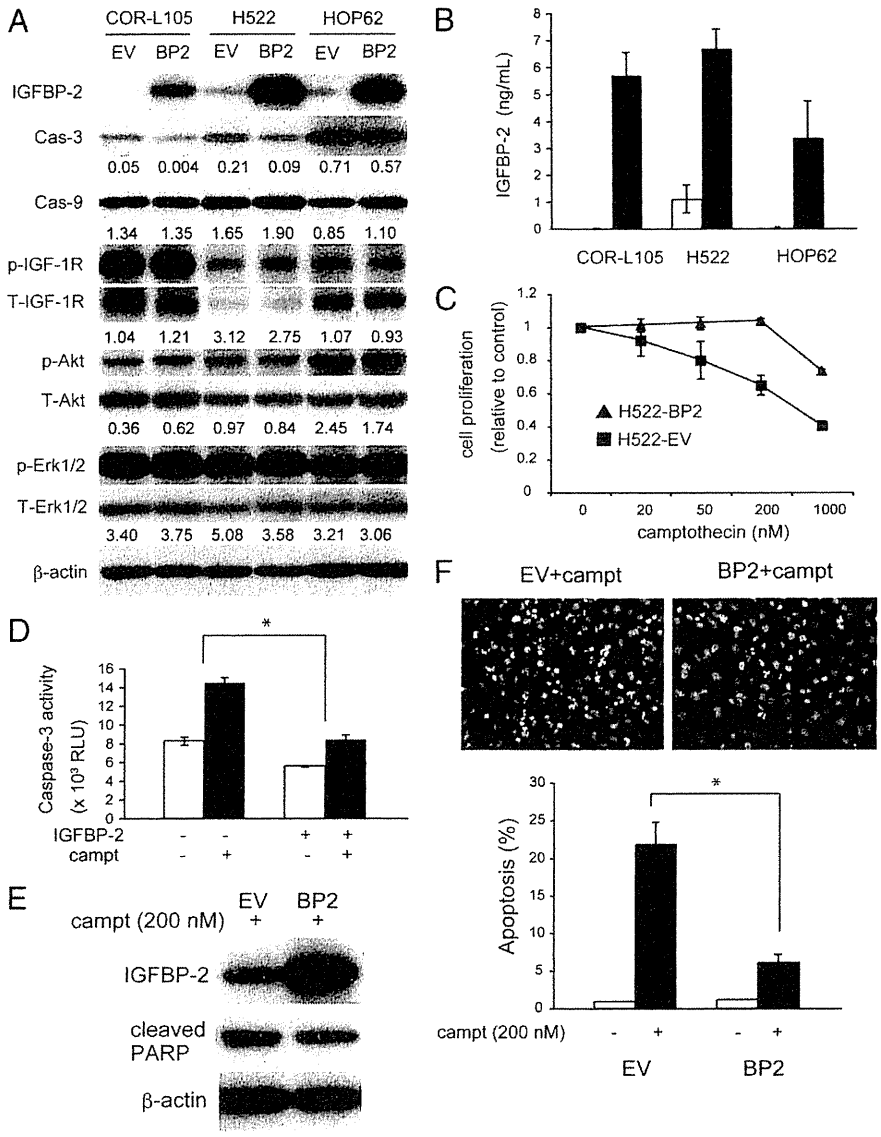

Figure 3. A: IGFBP-2 overexpression inhibits procaspase-3 expression independent of the IGF signaling pathway. Empty vector (EV) and IGFBP-2 (BP2) were transfected in COR-L105, NCI-H522, and HOP62 lung adenocarcinoma cell lines, and stably IGFBP-2 overexpressing cells were obtained. Whole cell lysates were subjected to SDS-polyacrylamide gel electrophoresis, followed by immunoblotting for IGFBP-2, procaspase-3, procaspase-9, phosphorylated and total IGF-1R, phosphorylated and total Akt, phosphorylated and total Erk1/2, and β-actin. Signal densities were quantified by ImageJ, and then procaspase-3/β-actin, procaspase-9/β-actin, p-IGF1R/T-IGF1R, p-Akt/T-Akt, and p-Erk1/2/T-Erk1/2 ratios were calculated. **B:** Secreted IGFBP-2 levels were measured by ELISA in three different stable vector- and IGFBP-2-transfected (white and black bars, respectively) cell lines. Data represent means ± SD. **C:** IGFBP-2 overexpressing and empty vector NCI-H522 cells were plated in 96 wells and treated with indicated concentration of camptothecin for 24 hours. Cell proliferation was determined by microplate reader using cell count reagent. Data represent means ± SD. The IC50 values were 686 nmol/L and more than 1000 nmol/L in empty vector and IGFBP-2 cells, respectively. **D:** Caspase-3 assay in IGFBP-2 overexpressing and empty vector NCI-H522 cells. Cells were plated in 96 wells and treated with 200 nmol/L of camptothecin for 24 hours. Caspase-3 activity was determined by a microplate reader. Data represent means ± SD. Statistical analysis of comparison between empty vector and IGFBP-2 overexpressing cells was performed by Welch's *t*-test. EV (camptothecin/DMSO) versus BP2 (camptothecin/DMSO); $^*P < 0.02$. **E:** Apoptosis was also evaluated by immunoblotting for PARP cleavage with whole cell lysate. **F:** Twenty-four hours after exposure of 200 nmol/L of camptothecin, cells were stained with Hoechst 33342. Apoptotic and nonapoptotic cells were counted by microscopy at least in three different areas, and the apoptotic rate was represented. Values represent means ± SD. Statistical analysis was performed by Welch's *t*-test. $^*P < 0.01$.

a real-time RT-PCR and Western blotting. IGFBP-2 mRNA was significantly higher in tumors than in paired normal tissue, as examined by a real-time RT-PCR ($P = 0.021$; Figure 5A). A higher amount of IGFBP-2 protein was also frequently observed in tumor tissue compared with in paired normal tissue (Figure 5B).

Inverse Relationship between IGFBP-2 and Caspase-3 Expression

Finally, immunohistochemical analysis was performed on tissue microarray including 169 cases of lung adenocarcinoma. IGFBP-2 expression was mostly confined to cancer cells, whereas normal lung epithelium revealed very low or undetectable IGFBP-2 levels (Figure 6A, arrowheads). In most cases, IGFBP-2 was localized in cytoplasm of lung adenocarcinoma cells, as shown in Figure 6A. Membraneous IGFBP-2 expression was found in only 3 of 169 cases (1.8%; Figure 6B). IGFBP-2 was expressed in early precursor lesions, and its expression levels increased gradually as the lesions progress from benign (Figure 6C, arrows) to malignant cells (Figure 6C, arrowheads). In particular, a strong IGFBP-2 expression was found in cancer cells with high nuclear grade distinct from ones with low nuclear grade even within the same gland (Figure 6D). It should be noted that the mutually exclusive expression between IGFBP-2 (Figure 6E, left panel, arrowheads and Figure 6F, left panel, upper area) and procaspase-3 (Figure 6E, right panel, arrowheads and Figure 6F, right panel, lower area) was frequently observed in lung adenocarcinomas. To summarize the immunohistochemical data, a significant inverse correlation between the groups in the numbers of patients with IGFBP-2 and procaspase-3 expression was observed in lung adenocarcinomas (Table 1).

Discussion

The IGF signaling pathway plays a pivotal role in cellular proliferation, differentiation, survival, and metabolism.

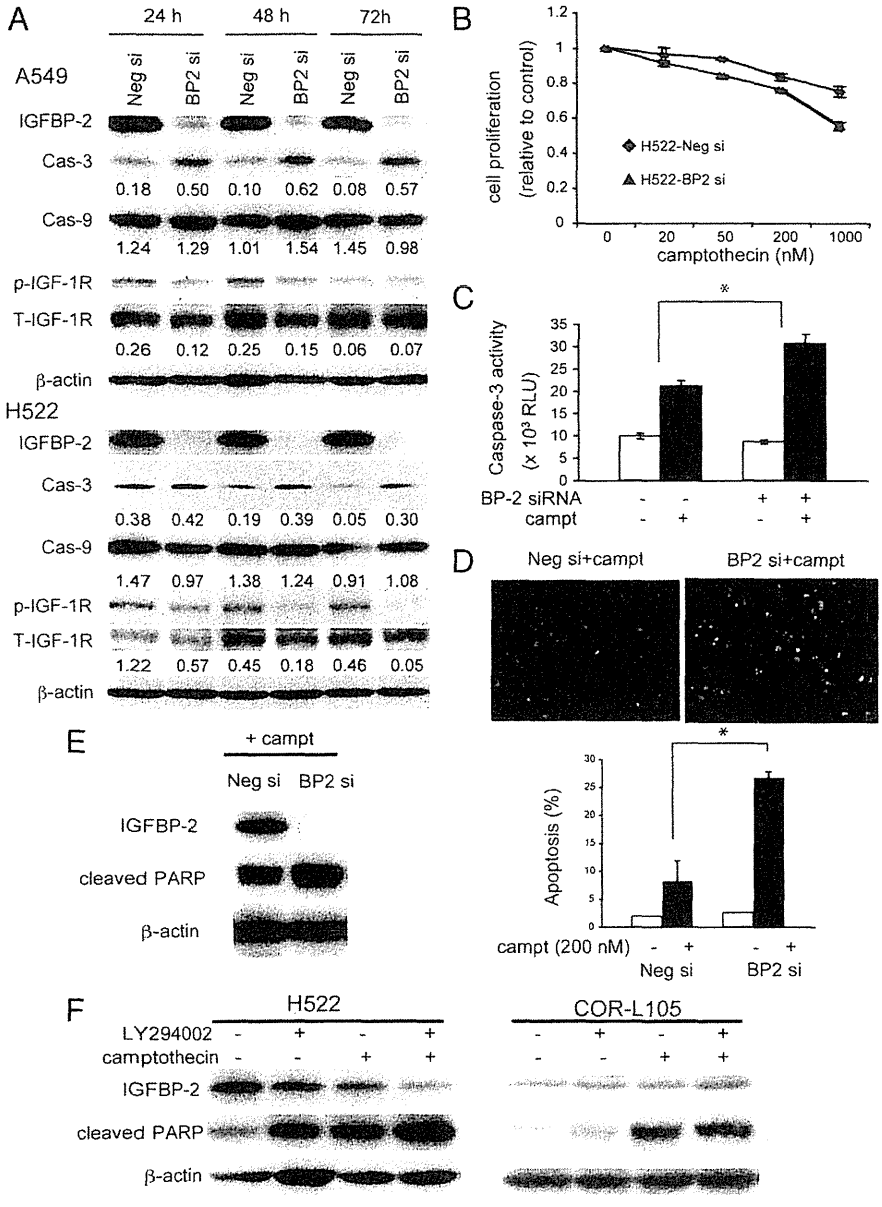

Figure 4. A: Specific IGFBP-2 inhibition resulted in the increase in procaspase-3. A549 or NCI-H522 cells were transfected with negative control or IGFBP-2 siRNA oligonucleotides, followed by immunoblot for IGFBP-2, procaspase-3, procaspase-9, phosphorylated and total IGF-1R, and β-actin at indicated times after transfection. Signal densities were quantified by ImageJ, and then procaspase-3/β-actin, Procaspase-9/β-actin, and p-IGF1R/T-IGF1R ratios were calculated. **B:** NCI-H522 cells were treated with negative control or IGFBP-2 siRNA for 24 hours and then exposed to different concentrations of camptothecin for 24 hours. Cell proliferation was determined as described before. Data represent means ± SD. A 95% CI based test of slope regression was significant ($P < 0.05$): −2.7E-04 to −1.6E-04 in negative siRNA vs. −4.5E-04 to −3.0E-04 in IGFBP-2 siRNA. **C:** Caspase-3 assay in NCI-H522 cells treated with negative control or IGFBP-2 siRNA. NCI-H522 cells were treated with negative control or IGFBP-2 siRNA for 48 hours in 96 wells and then treated with 200 nmol/L of camptothecin for 24 hours. Caspase-3 activity was determined by a microplate reader. Data represent means ± SD. Statistical analysis of comparison between negative control and IGFBP-2 siRNA was performed by Welch's *t*-test. $^*P < 0.0001$. **D:** Twenty-four hours after exposure of 200 nmol/L of camptothecin, siRNA-treated NCI-H522 cells were stained with Hoechst 33342. The apoptotic rate was measured as described previously. Values represent means ± SD. Statistical analysis was performed by Welch's *t*-test. $^*P < 0.001$. **E:** Apoptosis was also evaluated by immunoblot for PARP cleavage in NCI-H522 cells. **F:** NCI-H522 and COR-L105 cells were treated with 20 μmol/L of LY294002 or 200 nmol/L of camptothecin or combination of LY294002 and camptothecin for 24 hours. Immunoblot was performed with IGFBP-2, cleaved PARP, and β-actin antibodies.

IGFBPs are circulating proteins and function as modulators of IGF signaling through sequestration of IGFs in serum and the extracellular fluid. Increased levels of serum IGFBP-2 are found in certain pathophysiological conditions including fasting, diabetes mellitus, growth hormone deficiency, hepatic or renal failure, and cancer.[31] In cancer, IGFBP-2 exerts various biological functions by virtue of IGF-dependent or -independent mechanisms. Soluble IGFBP-2 binds to IGFs and consequently inhibits IGF signaling in various human cancers, including lung cancer.[19,32–34] Membrane-associated IGFBP-2 stimulates or inhibits cell proliferation and migration through a direct binding to serum and extracellular matrix molecules, such as cell surface integrin receptors, proteoglycans, and heparin.[2–5,35] Meanwhile, a number of studies demonstrate that intracellular IGFBP-2 promotes cancer cell growth in various cell types.[9,11,36] Moreover, IGFBP-2 overexpression confers resistance to apoptosis induced by chemotherapy in breast cancer cells[6] and by androgen ablation in prostate cancer.[9] Serum IGFBP-2 can be used for prediction of chemotherapy response and prognosis in ovarian cancer[37] and acute lymphoblastic leukemia.[38] Notably, IGFBP-2 is a marker for antiestrogen resistance, but not for cell growth in human breast cancer cells.[39] These observations invoke that intracellular IGFBP-2 mainly contributes to cancer cell survival independently of secreted IGFBP-2.

In the present study, we have shown that (1) intracellular IGFBP-2 regulates caspase-3 expression in an IGF independent manner; (2) IGFBP-2 overexpression prevents camptothecin-induced apoptosis, whereas IGFBP-2 inhibition promotes apoptosis; and (3) there is an inverse expression pattern between intracellular IGFBP-2 and caspase-3 in human lung adenocarcinomas.

We demonstrated a novel mechanism of antiapoptotic effect of IGFBP-2 via procaspase-3 inhibition in lung can-